Neurobiology of Disease

Slo2/K_{Na} Channels in *Drosophila* Protect against Spontaneous and Induced Seizure-like Behavior Associated with an Increased Persistent Na^+ Current

Nathan Byers, Eu-Teum Hahm, and Susan Tsunoda
Department of Biomedical Sciences, Colorado State University, Fort Collins, Colorado 80523

Na^+ sensitivity is a unique feature of Na^+-activated K^+ (K_{Na}) channels, making them naturally suited to counter a sudden influx in Na^+ ions. As such, it has long been suggested that K_{Na} channels may serve a protective function against excessive excitation associated with neuronal injury and disease. This hypothesis, however, has remained largely untested. Here, we examine K_{Na} channels encoded by the *Drosophila Slo2* (*dSlo2*) gene in males and females. We show that dSlo2/K_{Na} channels are selectively expressed in cholinergic neurons in the adult brain, as well as in glutamatergic motor neurons, where dampening excitation may function to inhibit global hyperactivity and seizure-like behavior. Indeed, we show that effects of feeding *Drosophila* a cholinergic agonist are exacerbated by the loss of dSlo2/K_{Na} channels. Similar to mammalian Slo2/K_{Na} channels, we show that dSlo2/K_{Na} channels encode a TTX-sensitive K^+ conductance, indicating that dSlo2/K_{Na} channels can be activated by Na^+ carried by voltage-dependent Na^+ channels. We then tested the role of dSlo2/K_{Na} channels in established genetic seizure models in which the voltage-dependent persistent Na^+ current (I_{Nap}) is elevated. We show that the absence of dSlo2/K_{Na} channels increased susceptibility to mechanically induced seizure-like behavior. Similar results were observed in WT flies treated with veratridine, an enhancer of I_{Nap}. Finally, we show that loss of dSlo2/K_{Na} channels in both genetic and pharmacologically primed seizure models resulted in the appearance of spontaneous seizures. Together, our results support a model in which dSlo2/K_{Na} channels, activated by neuronal overexcitation, contribute to a protective threshold to suppress the induction of seizure-like activity.

Key words: bang-sensitive; *Drosophila*; epilepsy; K_{Na} channels; seizure; Slo2

Significance Statement

Slo2/K_{Na} channels are unique in that they constitute a repolarizing K^+ pore that is activated by the depolarizing Na^+ ion, making them naturally suited to function as a protective "brake" against overexcitation and Na^+ overload. Here, we test this hypothesis *in vivo* by examining how a null mutation of the *Drosophila Slo2* (*dSlo2*)/*K_{Na}* gene affects seizure-like behavior in genetic and pharmacological models of epilepsy. We show that indeed the loss of dSlo2/K_{Na} channels results in increased incidence and severity of induced seizure behavior, as well as the appearance of spontaneous seizure activity. Our results advance our understanding of neuronal excitability and protective mechanisms that preserve normal physiology and the suppression of seizure susceptibility.

Introduction

Neuronal hyperactivity and Na^+ overload are associated with many neuropathological conditions, including Alzheimer's disease (Hartley et al., 1999; Palop et al., 2007; Busche et al., 2008, 2012; Kuchibhotla et al., 2008; Minkeviciene et al., 2009; J. T. Brown et al., 2011; Davis et al., 2014; Ping et al., 2015; Hahm et al., 2018), neuropathic pain (Calvo et al., 2019), amyotrophic lateral sclerosis (Kuo et al., 2004; Gunes et al., 2020), Fragile X Syndrome (Gibson et al., 2008; Deng and Klyachko, 2021), ischemia (J. M. Lee et al., 1999; Choi, 2020), traumatic brain injury (Huttunen et al., 2018), and epilepsy (Fisher et al., 2005). K^+ channels offer a fast response element to repolarize the membrane potential and prevent overexcitation. Na^+-activated K^+ (K_{Na}) channels, in particular, could provide the first line-of-defense against a sudden increase in intracellular Na^+ that occurs during neuronal injury and disease. Indeed, physiologists initially reported that high levels of

Received May 20, 2021; revised Aug. 20, 2021; accepted Sep. 13, 2021.

Author contributions: N.B., E.-T.H., and S.T. designed research; N.B., E.-T.H., and S.T. performed research; N.B., E.-T.H., and S.T. analyzed data; N.B. and S.T. wrote the first draft of the paper; N.B., E.-T.H., and S.T. edited the paper; S.T. wrote the paper.

This work was supported by the National Institutes of Health R01GM083335 to S.T. and R03NS109495 to S.T. We thank Drs. Mark Tanouye, Fengqui Diao, Benjamin White, Patrick Dolph, Lawrence Salkoff, and Diane O'Dowd for plasmids and fly lines.

The authors declare no competing financial interests.

Correspondence should be addressed to Susan Tsunoda at susan.tsunoda@colostate.edu.

https://doi.org/10.1523/JNEUROSCI.0290-21.2021

intracellular Na^+ (20-180 mM) were required to activate K_{Na} channels and suggested that they play a protective role during epileptic, ischemic, or hypoxic conditions (Kameyama et al., 1984; Luk and Carmeliet, 1990; Mitani and Shattock, 1992; Jiang and Haddad, 1993; Dryer, 1994; Yuan et al., 2003). Since the *Slo2.2/Slack/KCNT1/K_{Na}1.1* and *Slo2.1/Slick/KCNT2/K_{Na}1.2* genes were identified to encode K_{Na} channels (Bhattacharjee et al., 2003; Yuan et al., 2003), referred to herein as Slo2/K_{Na} channels, they have been found to be widely expressed in the CNS (Bhattacharjee et al., 2002, 2005; Rizzi et al., 2016). Consistent with a protective role against overexcitation, mutations in the human *Slo2/K_{Na}* genes, *KCNT1* and *KCNT2*, have been linked to multiple forms of epilepsy (Heron et al., 2012; Ishii et al., 2013; Møller et al., 2015; Gururaj et al., 2017; Ambrosino et al., 2018; Mao et al., 2020).

Structure-function studies have shown that cytoplasmic cofactors and post-translational regulation can potentially shift Na^+ sensitivity of Slo2/K_{Na} channels to a more physiologically relevant range (Yuan et al., 2003; Tamsett et al., 2009; Huang et al., 2013) and knock-down/-out studies of *Slo2.1/K_{Na}1.2* and *Slo2.2/K_{Na}1.1* in mice have demonstrated physiological functions of Slo2/K_{Na} channels. For example, Slo2/K_{Na} channels have been suggested to contribute to pain sensation and adaptation (M. R. Brown et al., 2008; R. Lu et al., 2015; Martinez-Espinosa et al., 2015; Evely et al., 2017; Tomasello et al., 2017), particular types of learning (Bausch et al., 2015; Quraishi et al., 2020), and locomotor (Quraishi et al., 2020) behaviors. Although a neuroprotective role against overexcitation and physiological roles in signaling are not mutually exclusive, the hypothesis that Slo2/K_{Na} channels serve as a built-in mechanism against Na^+ overload has remained largely untested.

Here, we use *Drosophila* as a model to test whether Slo2/K_{Na} channels protect against overexcitation. We examine the expression of the single *Drosophila Slo2* (*dSlo2*)/*K_{Na}* gene, then show that dSlo2/K_{Na} channels carry a TTX-sensitive K^+ current in cholinergic neurons that protects against behavioral abnormalities and seizure-like activity associated with prolonged exposure to a cholinergic agonist. Since our results suggest that dSlo2/K_{Na} channels are activated by the persistent Na^+ current (I_{Nap}), similar to Slo2/K_{Na} in mammalian neurons (Budelli et al., 2009; Hage and Salkoff, 2012), we examine the role of dSlo2/K_{Na} channels in genetic mutant and pharmacologically challenged backgrounds in which I_{Nap} has been elevated, leaving the organism prone to seizure induction. We show that loss of *dSlo2/K_{Na}* in these models increases the occurrence of induced seizure-like behavior, the severity of seizure-like behavior, as well as the number of individuals that exhibit spontaneous seizures.

Materials and Methods

Drosophila *strains*

w^{1118} was used as our WT control in this study. We used the previously generated mutations and transgenic insertions: *ChAT-GAL4* (BDSC #6798, 6013), *30y-GAL4, UAS-CD8-GFP, Dα1-T2A*-Gal4 (*nAchRα1^{Mi00453}-Gal4*, BDSC #6670), *para-RFP* (Ravenscroft et al., 2020), Δ*Mdr65* (Denecke et al., 2017a), *Mi13397* (Metaxakis et al., 2005; Venken et al., 2011), *vas-cas9* (BDSC #51323), Generalized Epilepsy with Febrile Seizures Plus (*GEFS$^+$*) (Sun et al., 2012) (gift from Diane O'Dowd), *bang-senseless* (*bss^1*) originally denoted (*bas^{MW1}*; gift from Mark Tanouye) (Jan and Jan, 1978), *julius seizure$^{iso7.8}$* (*jus$^{iso7.8}$*) previously known as *slamdance$^{iso7.8}$* (*sda$^{iso7.8}$*) (Zhang et al., 2002; Horne et al., 2017) (gift from Mark Tanouye), *easily shocked* (*eas^{PC80}*) (Ganetzky and Wu, 1982) (gift from Mark Tanouye), *SK$^-$* (Abou Tayoun et al., 2011) (gift from Patrick Dolph), *Sh^{ks133}*(Ganetzky and Wu, 1982); the following stocks, *ChAT-T2A*-LexA (*ChAT^{Mi04508}-LexA*), *GAD1-T2A-LexA (GAD^{Mi09277}-LexA), VGlut-T2A-LexA* (*VGlut^{Mi04979}-LexA), LexAop-TdTom-nls, UAS-2xEYFP, pC(lox2-attB2-SA-T2A-Gal4-Hsp70)3, hs-Cre,* and *vas-ΦC31*, were all from Diao et al. (2015) (gift from Benjamin White). Unless noted as a gift, remaining stocks were obtained from the Bloomington *Drosophila* Stock Center (as noted). The following lines were generated and used in the current study: *dSlo2/K_{Na}^-*, *dSlo2-T2A-Gal4, dSlo2-myc, UAS-dSlo2/K_{Na}, UAS-dSlo2/K_{Na}-DN*.

dSlo2/K_{Na}^- *null mutant*

CRISPR-Cas9 approaches, described previously (Gratz et al., 2015a, b), were used to generate the null mutant *dSlo2/K_{Na}^-*. To target the pore region, sequence spanning the S5-S6 transmembrane region was inserted into the online tool: http://tools.flycrispr.molbio.wisc.edu/targetFinder. Primers that include two gRNA sequences (underlined) to target upstream (forward: 5′-*CTT CGT GCT GGA TAC CAC AAA CGC*-3′; reverse: 5′-*AAA CGC GTT TGT GGT ATC CAG CAC*-3′) and downstream (forward: 5′-*CTT CGA TGA CCA TAT AAA GCT GCG*-3′; reverse: 5′-*AAA CGC CAG CTT TAT ATG GTC ATC*-3′) sequences flanking the *dSlo2/K_{Na}* pore. Primers were annealed, phosphorylated, and ligated into *pU6-BbsI-chiRNA* vector. A donor plasmid that would incorporate a screenable *3xP3≫DsRed* marker into the deleted site was designed for homology directed repair. Primers for the left homologous arm (forward: 5′- *TAC TCA CCT GCT ACT TCG CCA CTC AAC TGA CCC AAA TTC* -3′; reverse: 5′- *TAC TCA CCT GCT ACT CTA CCG CTG GGG ATA AAT AAA AAA* -3′), and right homologous arm (forward: 5′- *TAC TGC TCT TCA TAT AGC TTT ATA TGG TCA TCA TG* -3′; reverse: 5′- *TAC TGC TCT TCA GAC ATT ATT GGG CGG GTC CCA GA* -3′). Genomic DNA was isolated by standard phenol-chloroform extraction methods, followed by isopropanol precipitation. PCR using the left homologous arm primers and right homologous arm primers generated two separate products, which were ligated into the *pHD-DSRed-attp* vector using *AarI* and *SapI* restriction sites, respectively. gRNA and donor plasmids were microinjected into *vas-cas9* flies (Rainbow Transgenic Flies). Injected flies were crossed to w^{1118}, and progeny were screened for integration of the donor plasmid. Lines with successful deletion of *dSlo2/K_{Na}* pore sequence, indicated by expression of *DsRed* in the eye, were balanced by standard genetic approaches. *dSlo2/K_{Na}^-* null lines were verified by RT-PCR and DNA sequencing.

UAS-dSlo2/K_{Na} *transgenic lines*

dSlo2/K_{Na} cDNA (kindly provided by Lawrence Salkoff) was digested from the *pOX-dSlo2/K_{Na}* plasmid using KpnI and XhoI sites and ligated into the *pENTR1A* vector by Genewiz. The *pENTR1A-dSlo2/K_{Na}* vector was recombined with the *pTW* vector using Gateway Technology LR Recombination, and confirmed by DNA sequencing. *pTW-dSlo2* was injected into w^{1118} embryos (Rainbow Transgenic Flies). Transgenic lines were identified and isolated and by standard techniques. Positive *UAS-dSlo2/K_{Na}* insertions were driven by *elav-Gal4* and overexpression of *dSlo2/K_{Na}* was confirmed by RT-PCR.

UAS-dSlo2/K_{Na}-DN *transgenic lines*

dSlo2/K_{Na}-DN sequence was generated, in which sequence encoding the pore was mutated from a glycine-tyrosine-glycine (5′-*GGA TAC GGC*-3′) to alanine-alanine-alanine (5′-*GCC GCC GCC*-3′) (*GYG>AAA*). A larger sequence encompassing this mutant pore sequence was generated (Genewiz), digested at endogenous *DpnIII* and *ScaI* restriction sites, ligated into the digested *pENTR1A-dSlo2/K_{Na}* vector, and confirmed by DNA sequencing. *pENTR1A-dSlo2-DN* was recombined with the *pTW* vector using Gateway Technology LR Recombination to generate *pTW-dSlo2/K_{Na}-DN*, which was injected into w^{1118} embryos (Rainbow Transgenic Flies). Transgenic lines were isolated and identified by standard techniques, and *Gal4*-driven expression of *dSlo2-DN* was confirmed by RT-PCR.

dSlo2-T2A-Gal4 *line*

The Minos-Mediated Integration Cassette line *Mi13397* was used as a target for Trojan-mediated expression of *Gal4* (*T2A-Gal4*) that would be under the control of endogenous *dSlo2/K_{Na}* regulatory elements. *Mi13397* is located in a 5′ intronic region of all predicted splice forms of *dSlo2/K_{Na}*. Transgenic flies containing all three phases of *T2A-Gal4*, flanked by *attB* sites as well as *loxP* sites, were crossed to the *Mi13397* line, as described by Diao et al. (2015). Progeny were crossed to a line

expressing *hs-Cre* as well as *vas-ΦC31-Integrase*. Progeny from this cross were crossed to transgenic *UAS-EYFP* lines and screened for expression of EYFP, which would indicate successful insertion in the correct phase. EYFP-positive progeny were backcrossed to build a stable stock, and successful insertion of *T2A-Gal4* was further verified by DNA sequencing.

dSlo2-T2A-LexA *line*

The *T2A-LexA* cassette was inserted into the *Mi13397* site to create the *dSlo2-T2A-LexA* line. To allow for proper translation of *LexA*, the phase of the *Mi13397* insertion in the *dSlo2/K_{Na}* locus was predicted using the online tool (http://flypush.imgen.bcm.tmc.edu/pscreen/mimic.html) and confirmed to be Phase 2 by DNA sequencing. The plasmid *pBS-KS-attB2-SA(2)-T2A-LexA:QFAD-Hsp70* (kindly provided by Ben White) (Diao et al., 2015) was microinjected with the *vas-ΦC31* integrase plasmid into *Mi13397* embryos. Individually injected flies were crossed to *LexAop-TdTom-nls* flies, and progeny were screened for TdTom fluorescence.

dSlo2-myc *line*

A position in Exon 5 (immediately following nucleotide 94 of Exon 5) near the 3′ end of *dSlo2* was chosen for insertion *myc*. Optimal guide RNA (gRNA) target sites within Exon 5 were identified using the online tool (http://tools.flycrispr.molbio.wisc.edu/targetFinger/). Based on these results, a sense primer 5′-*CTT CGT TCT GCT CGA ACA TCA ACC* -3′ and antisense primer 5′- *AAA C<u>GG TTG ATG TTC GAG CAG AAC</u>* -3′ encoding the gRNA sequence (underlined) were annealed, phosphorylated, and ligated into the *BbsI* sites in *pU6-BbsI-chiRNA*. A single-stranded oligodeoxynucleotide (ssODN) repair template was designed such that the *myc* sequence (*GAA CAA AAA CTC ATC TCA GAA GAG GAT CTG*) was in-frame with *dSlo2/K_{Na}* and flanked by homologous regions of ~60 nt. Importantly, the *myc* sequence also disrupts the gRNA target sequence, preventing Cas9 digestion of the repair template. Both the *pU6-BbsI-chiRNA-Exon5* plasmid and ssODN were injected into *vas-Cas9* embryos (Rainbow Transgenic Flies). Individually injected flies were crossed to a double-balanced line, and progeny from these were backcrossed to each other. Once these flies began laying eggs, adults were pooled in groups of five and screened for successful insertion of the *myc* tag by PCR and restriction digest with *EarI*, a site located within the *myc* sequence. If digestion occurred, progeny from this vial were subsequently crossed individually to double-balancer lines. Once eggs were laid, the individual adult was screened for positive insertion. Successful insertion of in-frame *myc* sequence was ultimately confirmed by DNA sequencing.

Immunostaining and imaging

Larval body wall immunostaining. Larvae were fileted in cold PBS along the dorsal midline with slight cuts made perpendicular at each end. Corners of the body wall were pinned down on Sylgard, and tissue inside of the larvae was removed. The fileted prep was washed 3× in cold PBS, then fixed in 4% PFA in PBS for 30 min at room temperature. PFA was washed out 3 times with PBS. The prepared larval body wall was then blocked in PBS with 0.5% Triton-X 100 (PBT) and 5% BSA for 2-3 h, then incubated for ~48 h at 4°C on rocker in PBT with 5% BSA and primary mouse anti-myc (Santa Cruz Biotechnology, 9E10) at 1:50. Body walls were washed 3 times for 30 min, each in PBT with 5% BSA, then incubated in secondary goat anti-mouse conjugated to AlexaFluor-647 at 1:2000 overnight at 4°C. Body walls were again washed 3 times for 30 min in blocking solution, washed 2 times in PBS, followed by fixation in 4% PFA for 10 min to secure antibodies to their targets. Body walls were then washed in PBS, then H_2O, and mounted in VectaShield.

CNS immunostaining. Adult and larval *Drosophila* CNSs were dissected in cold PBS. Following dissection, CNSs were fixed in 4% PFA in PBS at room temperature for 20 min, washed 2 times in PBS, and 2 times in PBT. Primary antibodies used were mouse anti-myc (1:50, Santa Cruz Biotechnology), chicken anti-GFP (1:2000, Aves Labs), and rabbit anti-RFP (1:2000, Rockland Immunochemicals). Primary antibodies were diluted in PBT with 5% BSA or NGS and incubated with CNSs for 48-72 h at 4°C on rocker. CNSs were then washed 3× times in PBT for 10 min each. Alexa fluorophores, anti-chicken 488, anti-rabbit 568, and anti-mouse 647 from Invitrogen were used at a 1:2000 dilution in PBT with 5% BSA or NGS and incubated with CNS for 24-48 h at 4°C on rocker. CNSs were again washed three 3 times for 10 min each in PBT, washed 2 times in PBS, and fixed in 4% PFA for 10 min to secure antibodies to their targets. Following fixation, CNSs were rinsed in PBS, then H_2O, and mounted using Vectashield or DABCO (90% glycerol in PBS and 2.5% DABCO). Larval brains were oriented with the dorsal side facing the coverslip, whereas the adult brains were oriented with the ventral side facing the coverslip.

Images were acquired on either an upright Zeiss LSM 880 fluorescence confocal microscope or an inverted Zeiss LSM 800 fluorescence confocal microscope (Carl Zeiss). *Z* stacks and image tiling on the Zeiss ZEN software were used to acquire images of whole brains. Images were processed in ImageJ, and maximum intensity *Z* projections were generated when compiling *Z*-stack images.

Immunostaining embryonic cultures. Single embryos aged 5-6 h (at room temperature) were dissociated in drop cultures of 20 μl culture medium, as previously described (Tsunoda and Salkoff, 1995a, b; Eadaim et al., 2020). After overnight primary antibody incubation at 4°C, cultures were washed, and incubated with secondary. Cultures were fixed in 4% formaldehyde in PBS for 10 min, blocked (1% BSA or 5% goat serum, 0.1% saponin in PBS) for 30 min, then incubated with primary antibody overnight at 4°C. Antibodies against the following proteins were used at the indicated concentrations: anti-myc (1:50; c-Myc Antibody (9E10), Santa Cruz Biotechnology), anti-RFP (1:2000; Rockland). After 4 washes (0.1% saponin in PBS, 5 min each), we incubated cultures with goat-anti-rabbit/mouse AlexaFluor-568/-488 (1:500-1000; Invitrogen) secondary antibodies at room temperature for 2 h, washed again, then mounted them in p-phenylenediamine in 90% glycerol. We imaged cultures with a 60× oil-immersion objective, using Zeiss Apotome technology to obtain optical sections. Images were acquired with Zen Blue (2012) software (Zeiss) and processed for figures using Adobe Photoshop and Illustrator.

Imidacloprid feeding

Larval feeding was performed as previously described (Perry et al., 2008, 2012; Somers et al., 2015). An insecticide containing the active ingredient imidacloprid ("Compare N Save Systemic Tree and Shrub Insect Drench," Ragan & Massey) was diluted 1:1000 in H_2O. From this dilution, imidacloprid was added to standard cornmeal and agar food at the listed concentrations and allowed to solidify overnight in the dark. Embryos were collected from adult flies on egg laying plates of grape juice and agar. Embryos were aged for 24 h to the L1 larval stage. Twenty L1 larvae were gently collected from the egg laying plates using a brush and placed on the cornmeal and agar food containing different concentrations of the insecticides. Larvae were aged for 14-18 d in the dark to prevent degradation of the drug by exposure to light. The larvae that made it to adulthood were counted and averaged over three separate feeding trials, each with three vials (20 larvae/vial) per genotype.

Acute exposure assays following eclosion were performed similar to a previously described study (Denecke et al., 2017b), with noted adjustments. Media containing 5% sucrose and 1% agar were boiled to dissolve sucrose and agar, then imidacloprid was added to final concentration and stirred thoroughly; 4 ml of the food mixture was then aliquoted into separate vials and allowed to solidify overnight in the dark. Newly eclosed males (<24 h) were collected and aged for 5 d under 12 h light/12 h dark conditions. On the fifth day, flies were starved in empty vials for 4 h. Flies were then placed in the imidacloprid food mixture vials and left in the dark. Every 24 h, flies were analyzed for their ability to stand, walk, or groom. If flies were unable to stand or walk, or were dead, they were counted as "affected."

For imidacloprid feeding before mechanical stimulation, powdered imidacloprid (Sigma-Aldrich, #138261-41-3) was dissolved in H_2O to make a 2.36 mM stock solution and kept in the dark. Dissolved imidacloprid was added to media (5% sucrose + 1% agar) to a final concentration of 9 ppm. Male flies were aged for 3 d under 12 h light/12 h dark conditions. On the morning of the third day, flies were placed on the mock- or imidacloprid-food for 24 h under 12 h light/12 h dark conditions. Flies were then subjected to bang-sensitive assays blinded to the

researcher. Groups of 5 flies were transferred to empty vials and allowed to acclimate for at least 5 min, then were subjected to 30 s of vortex at high speed. Immediately following vortex, flies were analyzed to determine the fraction that were paralyzed. Fractions affected were averaged across multiple trials.

Veratridine feeding

Newly eclosed male flies (5 per vial) rested, following CO_2 exposure, for 24 h under 12 h light/12 h dark conditions. Flies were then starved for 24 h (25°C, ~64% humidity) in empty vials containing only H_2O-soaked filter paper. The H_2O-soaked filter paper was replaced with filter paper soaked in 2% sucrose containing either 20 μM veratridine (V-110, Alomone Labs) in DMSO or the vehicle ("mock"; 0.05% DMSO) and left for 2 h. Flies were then tested in mechanically induced and spontaneous seizure assays.

Mechanically induced seizure assays

Newly eclosed male flies were aged for 2 d under 12 h light/12 h dark conditions, gently transferred individually to empty vials using a suction pipette to avoid the use of CO_2. Flies were allowed to acclimate to the new vials for at least 5 min, then subjected to a 10 s vortex on high speed. Immediately following vortex, flies were videotaped for later analysis offline. The time to each behavioral characteristic was noted by the researcher, who was blinded to the genotype. These characteristics included the time to both the recovery seizure and full recovery; seizure was characterized by the inability to stand or walk and/or uncontrollable motor function. Additionally, flies were scored for a secondary paralysis period, characterized by a period of quiescence following the recovery seizure that lasted for at least 3 s. If flies exhibited a secondary paralysis, the time spent paralyzed was also measured. These characteristics were averaged across trials of ~20 flies individually assayed for each genotype.

Heat-induced seizure assays

In experiments using the $GEFS^+$ line, newly eclosed females were aged for 2-3 d. To induce seizures, 5 flies were placed in empty vials and allowed to acclimate for at least 5 min. Flies were then placed in a 40°C water bath, and behavior was videotaped. Analysis of recordings was done offline with the researcher blinded to the genotype of the flies. Seizure-like behavior, defined as uncontrolled motor behavior or paralysis, was scored as a fraction of the total flies every 10 s per vial and averaged across trials.

Spontaneous seizure assays

Newly eclosed male flies were placed in vials in groups of 10 per vial and aged for 2 d under 12 h light/12 h dark conditions. Before testing, flies were gently transferred to empty vials, allowed to acclimate to the new environment for 30 min, then videotaped for 15 min. Videos were analyzed offline, with the researcher blinded to the genotype. Seizures were characterized as random bouts of uncontrollable motor movement in which the flies were unable to stand or walk. The number of overall seizures exhibited in a vial were totaled over the 15 min period and averaged across genotypes.

Electrophysiological recordings

Whole-cell recordings were performed in perforated patch-clamp configuration by adding 400-800 μg/ml Amphotericin-B (Sigma-Aldrich) in the pipette, as described previously (Ping and Tsunoda, 2011; Ping et al., 2011). For Na^+ and K^+ current recordings, we used external solution (in mM) as follows: NaCl 140, KCl 2, HEPES 5, $CaCl_2$ 1.5, $MgCl_2$ 6, pH 7.2. For Na^+-free external solution, CholineCl was substituted for NaCl. For Na^+ current (only) recordings, we used Cs-based internal solution composition (in mM) as follows: CsCl 10, Cs-methanesulfonate 130, HEPES 10, EGTA 0.5, ATP-Mg 4, $MgCl_2$ 2, $CaCl_2$ 0.1, pH 7.2. Electrodes were filled with internal solution (in mM) as follows: K-gluconate 120, KCl 20, HEPES 10, EGTA 1.1, $MgCl_2$ 2, $CaCl_2$ 0.1, ATP-Mg 4, pH 7.2. All recordings were performed at room temperature. Gigaohm seals were obtained for whole-cell recordings. Data were acquired and analyzed using an Axopatch 200B amplifier, Axon Digidata 1440A, and pClamp 10.7 software (Molecular Devices). Recordings were digitized at 5 kHz and filtered at 2 kHz, using a lowpass Bessel filter. Additional analysis and presentation software used for all electrophysiological data include the following: Clampfit 10.7 (Molecular Devices), Origin (Microcal Software), and Illustrator (Adobe). Averaged data presented as mean ± SEM. $p < 0.05$ (Student's t test).

TTX (Sigma-Aldrich) and veratridine (Alomone Labs) were prepared in stock solutions of 2 and 50 mM, respectively. Veratridine was dissolved in DMSO for stock solution, then added to external solutions at final concentrations indicated in the text, and the vehicle concentrations did not exceed 0.01%. Drugs were applied using a rapid application system, termed the "Y-tube method," which can change the local external solution within a few seconds, as described previously (Akaike et al., 1991; Min et al., 1996).

Experimental design and statistical analyses

In these studies, male *Drosophila* were used for all comparisons except for those made with $bss^{-/+}$ mutants (see Figs. 5, 6, and 8); because the *bss* gene is on the X chromosome, heterozygous bss^- required that we use females. Sample sizes and controls are indicated in the figure legends. All behavioral experiments were performed in multiple cohorts with genotypes blinded to the experimenter, as described in Materials and Methods for each experimental assay. Reported are mean ± SEM values, and the standard statistical test used was the unpaired two-tailed t test. The criterion used for statistical significance was $p < 0.05$; lesser values (e.g., $p < 0.01$) are also noted in the figure legends.

Results

dSlo2/K_{Na} channels are expressed in excitatory neurons in the CNS

To first examine where *dSlo2/K_{Na}* is expressed in the CNS, we set out to generate a transgenic line expressing the transcriptional activator Gal4 under the control of native *dSlo2/K_{Na}* regulatory elements. Using the previously developed "Trojan exon" system (Diao et al., 2015), we aimed to introduce a "Trojan exon," containing a splice acceptor site followed by the *T2A-Gal4* sequence, into a coding intron within the *dSlo2/K_{Na}* gene. When spliced into the *dSlo2/K_{Na}* coding transcript, the viral-based T2A signal is predicted to terminate translation of the *dSlo2/K_{Na}* transcript and promote translation of Gal4 as a second protein product from the same transcript (Diao and White, 2012; Diao et al., 2015; P. T. Lee et al., 2018). This results in Gal4 expression that should mimic endogenous *dSlo2/K_{Na}* expression (this will also result in truncation of *dSlo2/K_{Na}* just upstream of the S1 transmembrane domain, making it in effect a null mutant of *dSlo2/K_{Na}*). To generate this line, ΦC31-mediated recombination was used to induce an *in vivo* exchange of an exogenously provided *T2A-Gal4* cassette for a previously inserted Minos-Mediated Integration Cassette element (Venken et al., 2011), *Mi13397*; *Mi13397* is present in a coding intron predicted to be incorporated into all splice forms of *dSlo2*. Successful exchange of the *T2A-Gal4* cassette was screened for and verified by DNA sequencing; we refer to this new line as *dSlo2-T2A-Gal4*. We used *dSlo2-T2A-Gal4* to drive expression of *UAS-EYFP* or *UAS-CD8-GFP* as a reporter for *dSlo2/K_{Na}* expression in the larval and adult CNS.

In the CNS of third instar (L3) larvae, *dSlo2-T2A-Gal4≫UAS-EYFP* expression was most abundant in Kenyon cells (KCs) and cells in the ventral nerve cord (VNC) (Fig. 1*A*). In the adult CNS, we observed widespread *dSlo2/K_{Na}* reporter expression, with especially strong expression in KCs, and in the morphologically distinct motor neurons of the VNC (Fig. 1*B*). KCs have been shown to play a key role in associated visual and olfactory learning and memory function (Heisenberg et al., 1985; McGuire et al., 2001; Tanaka et al., 2008; van Swinderen, 2009). *dSlo2/K_{Na}* reporter expression was also found in second-order sensory processing cells, including the lamina and medulla of the

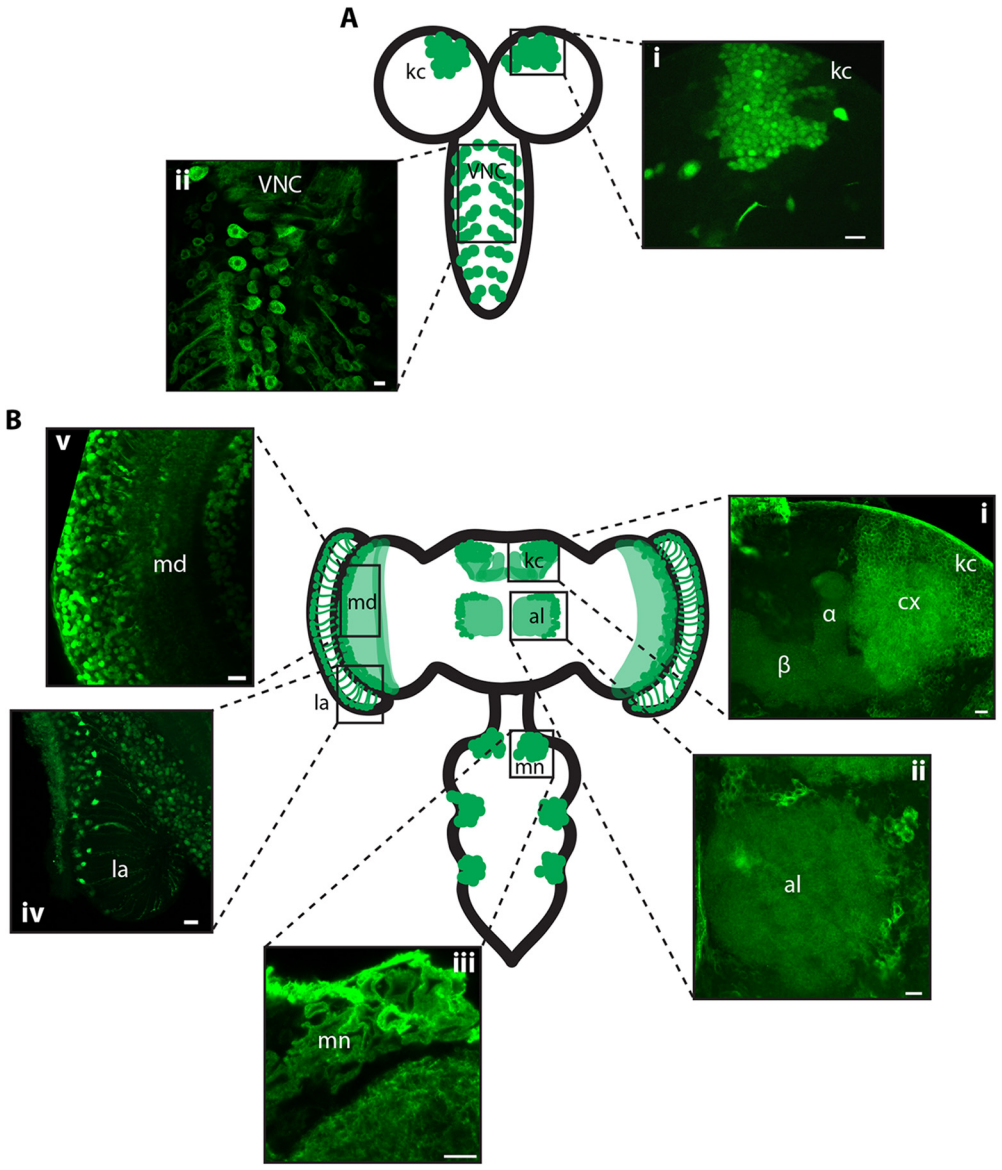

Figure 1. dSlo2/K_{Na} reporter expression in the larval and adult nervous system. ***A***, Representative optical sections, 0.6-0.8 μm, from an L3 larval brain show the following: (***Ai***) *dSlo2-T2A-Gal4≫UAS-EYFP* expression in KCs (kc) and (***Aii***) *dSlo2-T2A-Gal4≫UAS-mCD8-GFP* expression in the VNC. ***B***, Representative optical sections and *Z* projections from the adult brain are as follows: (***Bi***) *Z* projection of 27 confocal sections spanning 16.5 μm showing *dSlo2-T2A-Gal4≫UAS-mCD8-GFP* expression in KCs (kc), calyx (cx), and mushroom body lobes (α and β); (***Bii***) *Z* projection of 7 confocal sections spanning 3.5 μm showing *dSlo2-T2A-Gal4≫UAS-mCD8-GFP* expression in the antennal lobe (al); (***Biii***) optical sections, 0.6-0.8 μm, showing *dSlo2-T2A-Gal4≫UAS-mCD8-GFP* expression in motor neurons (mn); (***Biv***) optical sections, 0.6-0.8 μm, showing *dSlo2-T2A-Gal4≫UAS-EYFP* expression in the lamina (la) of the optic lobe; and (***Bv***) optical sections, 0.6-0.8 μm, showing *dSlo2-T2A-Gal4≫UAS-EYFP* expression in the medulla (md) of the optic lobe. Scale bars, 10 μm.

optic lobe, and the antennal lobe that receives input from olfactory receptor neurons (Fig. 1*B*). Thus, dSlo2/K_{Na} channels may function in regulating excitability in neurons involved in sensory processing, and learning and memory function.

Since *dSlo2/K_{Na}* expression appeared to be widespread, at least at low levels, we next investigated whether *dSlo2/K_{Na}* is preferentially expressed in cholinergic, GABAergic, and/or glutamatergic neurons. To do this, we used *ChAT-T2A-LexA*, *GAD1-T2A-LexA*, and *VGlut-T2A-LexA* lines, respectively, which drive LexA expression in each of these respective neuronal subtypes. *LexA* transgenes and *dSlo2-T2A-Gal4* were used to drive expression of different colored fluorophores in the same brains. *dSlo2-T2A-Gal4* drove expression widely in cholinergic neurons, as expected, since the major excitatory neurotransmitter in the *Drosophila* brain is acetylcholine (Fig. 2*A*). Since neurons localized to the medulla cortex exhibit a mixture of cholinergic and GABAergic neurons (Strother et al., 2017), we used this region to examine whether *dSlo2-T2A-Gal4* was expressed in excitatory and/or inhibitory neurons. Interestingly, all apparent *dSlo2-T2A-Gal4≫UAS-EYFP*-positive neurons were also positive for *ChAT-LexA≫LexAop-TdTomato-nls* (Fig. 2*A*). In contrast, *dSlo2-T2A-Gal4≫UAS-EYFP* and *Gad1-LexA≫LexAop-TdTomato-nls* were strikingly nonoverlapping (Fig. 2*B*), suggesting that dSlo2/K_{Na} channels are expressed exclusively in cholinergic neurons and excluded from GABAergic neurons. *dSlo2-T2A-Gal4≫UAS-CD8-GFP* expression in glutamatergic cells appeared to be cell type-specific. For example, in the medulla cortex of the optic lobe, *dSlo2-T2A-Gal4≫UAS-CD8-GFP* and *VGlut^{Mi14979}-LexA≫LexAop-TdTomato-nls* expression showed no apparent overlap, whereas in the VNC, significant overlap was observed in motor neurons (Fig. 2*C*). The widespread expression in excitatory neurons in the brain, and in motor neurons, suggests that dSlo2/K_{Na}

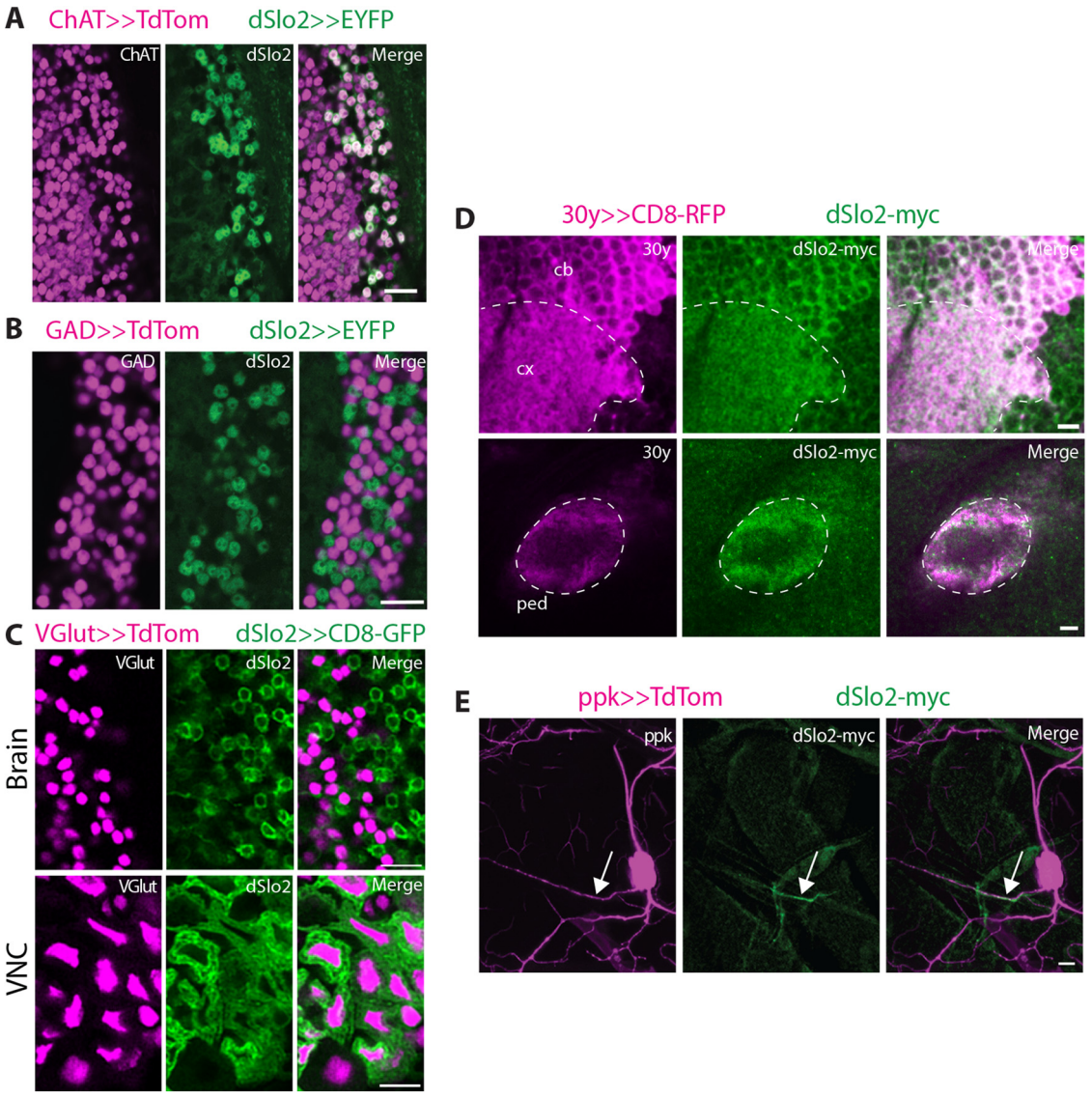

Figure 2. *dSlo2-T2A-Gal4* drives expression selectively in cholinergic neurons. ***A***, ***B***, Representative optical sections, 0.6-0.8 μm, of *UAS-EYFP* driven by *dSlo2-T2A-Gal4* (dSlo2≫EYFP; green) through the medulla cortex of the adult brain. *LexAop-TdTom-nls* (magenta) was simultaneously driven in (***A***) cholinergic neurons with *ChAT-T2A-LexA* (ChAT≫TdTom) and (***B***) GABAergic neurons with *Gad1-T2A-LexA* (GAD≫TdTom). ***C***, Representative optical sections, 0.6-0.8 μm, showing *dSlo2-T2A-Gal4≫UAS-mCD8-GFP* (dSlo2≫CD8-GFP, green) expression in glutamatergic neurons identified by expression of *VGlut-T2A-LexA≫UAS-TdTom-nls* (VGlut≫TdTom) in the medulla (top, Brain) and VNC (bottom). ***D***, Representative optical sections, 0.6-0.8 μm, showing *30y-Gal4≫UAS-CD8-RFP* (30y≫CD8-RFP; magenta) and *dSlo2-myc* (dSlo2-myc; green) coimmunolabeling in KCs (top, cell bodies [cb] and calyz [cx]) and in an optical cross-section of the peduncle (ped; dotted white outline). ***E***, *Z* projection of 19 confocal sections spanning 18 μm showing coexpression of *ppk-Gal4≫UAS-CD4-TdTom* (ppk≫TdTom; magenta) and *dSlo2-myc* (green) in Class IV multidendritic neurons. Arrows indicate axonal projection from this multidendritic neuron. Scale bars, 10 μm.

channels might function to modulate neuronal, and perhaps behavioral, excitability.

To gain further insight into how dSlo2/K_{Na} channels might function in neuronal excitability, we set out to characterize the subcellular localization of dSlo2/K_{Na} channels. To do this, we generated a line in which DNA coding for *myc* was inserted into the endogenous *dSlo2/K_{Na}* gene such that the translated myc epitope would be fused within the C-terminus of the channel subunits (see Materials and Methods); we refer to this line as *dSlo2-myc*. We found that dSlo2-myc was differentially localized to cell bodies and axonal/dendritic subcompartments in various neuronal subtypes. For example, in KCs, dSlo2-myc expression was localized to cell bodies, the calyx, and peduncle, a structure consisting of KC axons that project to the mushroom body lobes (Figs. 1*B* and 2*D*), but was absent from the axons in the mushroom body lobes themselves. Since the calyx consists of a mixture of dendritic processes from the KCs as well as axonal processes from other neurons, such as the projection neurons, it is unclear whether dSlo2-myc was present in the dendrites of the KCs and/or axonal terminals from projection neurons. We also examined the subcellular localization of dSlo2-myc in Class IV multidendritic neurons whose axonal and dendritic processes are clearly distinguishable. We found that dSlo2-myc channels were localized to axonal process of these neurons, but seemingly absent from dendrites and cell bodies (Fig. 2*E*). Thus, dSlo2-myc appears to be trafficked to different neuronal subcompartments, depending on cell identity, where these dSlo2/K_{Na} channels may dampen neuronal excitability by different mechanisms.

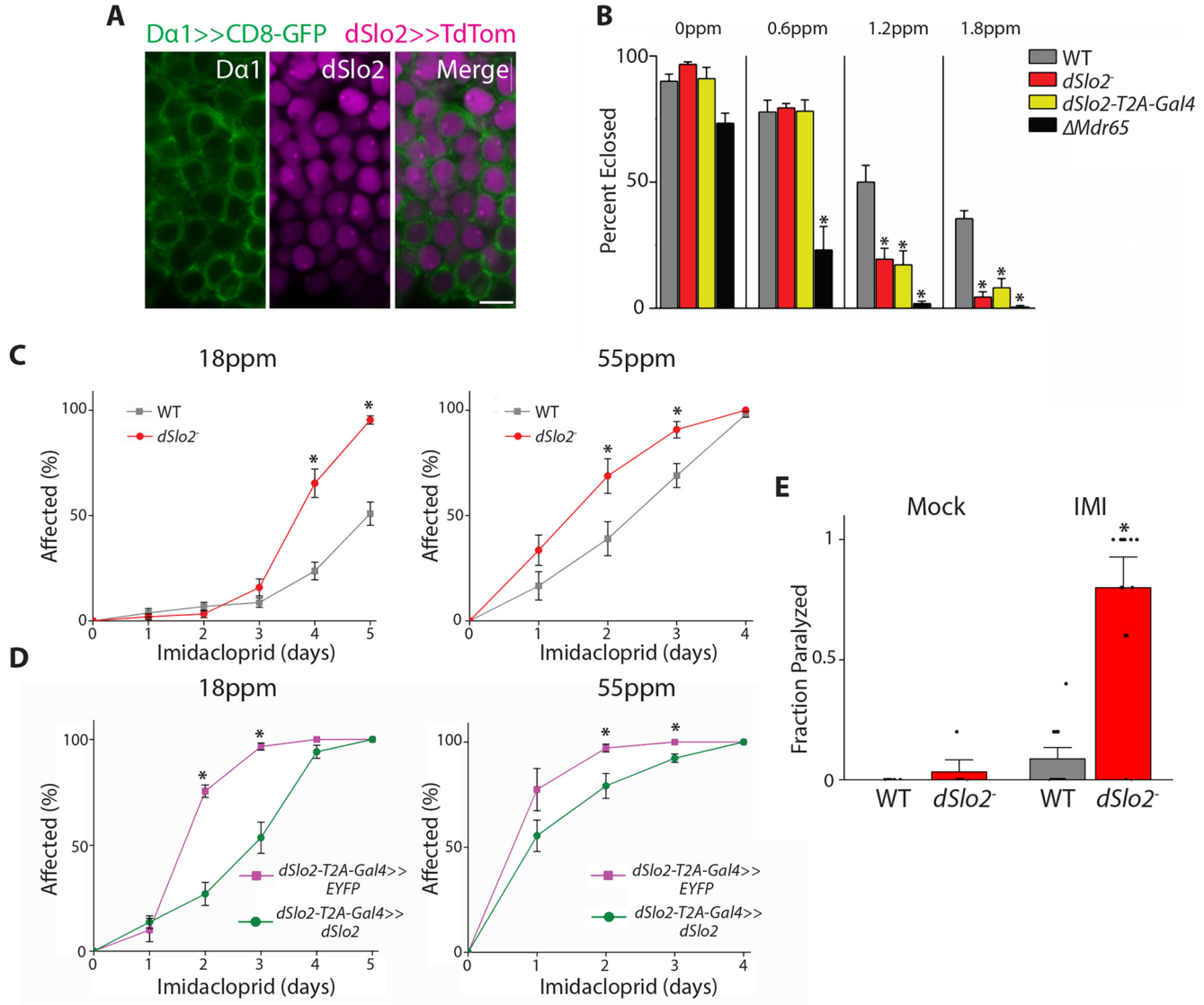

Figure 3. Effects of the cholinergic agonist, imidacloprid, are exacerbated in *dSlo2/K_{Na}*⁻ mutants. ***A***, Representative optical sections showing *UAS-CD8-GFP* and *LexAop-TdTom-nls* driven by *Dα1-Gal4* and *dSlo2-T2A-LexA*, respectively (Dα1≫CD8-GFP [green] and dSlo2≫TdTom [magenta]), in KC bodies of the adult brain. Scale bar, 10 µm. ***B***, Mean percentage of adults that eclosed from groups of 20 L1 larvae raised on food with containing 0, 0.6, 1.2, or 1.8 ppm imidacloprid. Genotypes are as indicated: WT, *dSlo2/K_{Na}*⁻ (*dSlo2*⁻), *dSlo2-T2A-Gal4*, and *ΔMdr65*. $n = 6$-9 groups per genotype. ***C***, ***D***, Mean percentage of flies scored as "affected" (inability to stand or walk; see Materials and Methods) was averaged each day following placement of flies on food containing either 18 ppm (left) or 55 ppm (right) imidacloprid. Genotypes are as indicated: WT and *dSlo2/K_{Na}*⁻ (***C***), and *dSlo2-T2A-Gal4* and *dSlo2-T2A-Gal4≫UAS-dSlo2* (***D***). $n = 8$-10 groups of 5 flies per group for each genotype. ***E***, Fraction of flies paralyzed following a 30 s mechanical stimulation (see Materials and Methods) after 24 h of feeding either vehicle (Mock) or 9 ppm imidacloprid (IMI). $n = 12$-16 trials of 5 flies per group for each condition and genotype. Data are mean ± SEM. *$p < 0.05$, mutant data compared with WT (Student's *t* test).

Effects of a cholinergic agonist are exacerbated by the loss of *dSlo2/K_{Na}* channels

Given the expression of *dSlo2/K_{Na}* in excitatory cholinergic neurons in the brain, and the likelihood that dSlo2/K_{Na} channels would be activated by increased excitation, our goal was to test the long-standing hypothesis in the field that Slo2/K_{Na} channels dampen excitability when confronted with excessive excitation (Kameyama et al., 1984). We first investigated whether dSlo2/K_{Na} channels might function in circumstances of increased excitation induced by feeding flies the cholinergic agonist, imidacloprid. Activation of nicotinic acetylcholine receptors (nAChRs), the major excitatory receptor in the *Drosophila* CNS, results in an influx of cations, including Na^+, which could in turn activate dSlo2/K_{Na} channels. Since we planned to feed flies imidacloprid, which has been shown to act as a partial agonist for Dα1 nAChRs (L. A. Brown et al., 2006; Perry et al., 2008; Ihara et al., 2018), we first confirmed that dSlo2/K_{Na} channels and Dα1 receptors have overlapping expression. To do this, we generated and used *dSlo2/K_{Na}-T2A-LexA* and *Dα1-T2A-Gal4* lines to drive expression of *LexAop-TdTomato-nls* and *UAS-CD8-GFP*, respectively. Throughout the CNS, we found that virtually all Dα1-positive cells were also positive for dSlo2/K_{Na} reporter expression (Fig. 3*A*).

We then examined the toxic effects of feeding WT larvae imidacloprid. We placed WT first instar (L1) larvae on food mixed with imidacloprid, which they consumed for the rest of development, then scored for the number of viable adults that eclosed. Consistent with earlier reports (Perry et al., 2008; Denecke et al., 2017b), we found that the fraction of larvae that survived to adulthood was progressively reduced as the concentration of imidacloprid was increased (Fig. 3*B*). We also tested *ΔMdr65* mutants, which contain a deletion of the *Mdr65* gene that

encodes an ATP-binding cassette transporter. These mutants were previously shown to be highly susceptible to imidacloprid treatment because of an inability to effectively efflux the compound from the CNS (Denecke et al., 2017a), and have been used here as a positive control for imidacloprid toxicity. Indeed, even at 0.6 ppm imidacloprid, only 23% of the Δ*Mdr65* larvae eventually eclosed as adults, compared with 78% of WT; at 1.2 ppm imidacloprid, only 1% of Δ*Mdr65* adults eclosed (Fig. 3*B*). Previous studies have shown that this imidacloprid toxicity is because of its hyperactivation of Dα1 nAChRs (Perry et al., 2008).

Hyperactivation of Dα1 nAChRs would likely result in an overload of intracellular Na^+, and perhaps activation of dSlo2/K_{Na} channels as a protective measure. To test whether the loss of dSlo2/K_{Na} channels would affect imidacloprid toxicity, we generated a *dSlo2/K_{Na}^-* null mutant line (see Materials and Methods) and examined whether *dSlo2/K_{Na}^-* mutants exhibited any difference in imidacloprid toxicity compared with WT. We found that indeed *dSlo2/K_{Na}^-* mutants were more sensitive to imidacloprid. At 1.2 and 1.8 ppm imidacloprid, 50% and 35% of WT flies eclosed, respectively, while only 18% and 6% of *dSlo2/K_{Na}^-* mutants eclosed, respectively (Fig. 3*B*). We also tested the *dSlo2-T2A-Gal4* line, which, as described above, is predicted to essentially be a null mutant of *dSlo2/K_{Na}*. We found that *dSlo2-T2A-Gal4* flies were also more susceptible to imidacloprid than WT flies (Fig. 3*B*). Our results show that imidacloprid toxicity during development is more detrimental in the absence of dSlo2 channels, suggesting that dSlo2 channels act protectively against imidacloprid-induced hyperactivity.

We next examined whether adult flies acutely fed imidacloprid exhibit detectable behavioral alterations. For these experiments, flies were fed food mixed with imidacloprid, then scored each day as "affected" if they were unable to walk, stand, or groom. We found that, after 3 d of feeding on 18 ppm imidacloprid or after 1 d of feeding on 55 ppm imidacloprid, an increasing number of WT flies were affected, with 100% of the flies affected after 4 d feeding on 55 ppm imidacloprid (Fig. 3*C*). When *dSlo2/K_{Na}^-* mutants were examined in concurrent assays, we found that significantly more *dSlo2/K_{Na}^-* mutants were affected than WT. This can be seen at 4-5 d on 18 ppm imidacloprid, and 2-3 d on 55 ppm imidacloprid (Fig. 3*C*). To test whether this increased susceptibility to imidacloprid was because of the loss of dSlo2/K_{Na} channels, we examined whether exogenous expression of *dSlo2/K_{Na}* in a *dSlo2/K_{Na}^-* mutant background would rescue the percent of flies affected by imidacloprid. To do this, we used the *dSlo2-T2A-Gal4* line as a *dSlo2/K_{Na}* loss-of-function background. Indeed, like the *dSlo2/K_{Na}^-* mutant, the *dSlo2-T2A-Gal4* line showed high sensitivity to imidacloprid (Fig. 3*D*); it is unclear why the *dSlo2-T2A-Gal4* line was even more sensitive to imidacloprid than *dSlo2/K_{Na}^-*. We generated *UAS-dSlo2/K_{Na}* transgenic lines to test for rescue of this increased sensitivity. We used *dSlo2-T2A-Gal4* to drive expression of *UAS-dSlo2/K_{Na}* (*dSlo2-T2A-Gal4≫UAS-dSlo2/K_{Na}*) and tested for imidacloprid susceptibility. We found that the percent of flies affected after 2-3 d on imidacloprid was indeed significantly reduced with expression of *UAS-dSlo2/K_{Na}* (Fig. 3*D*), suggesting that dSlo2/K_{Na} channels function protectively against imidacloprid-induced hyperactivity.

Since other hyperactive lines have been characterized to exhibit paralysis induced by mechanical stress (Parker et al., 2011b), we also tested whether mock- and imidacloprid-fed WT and *dSlo2/K_{Na}^-* flies exhibited any difference in mechanically induced paralytic behavior. We found that WT mock-treated flies and flies fed 9 ppm imidacloprid for 24 h showed no significant change in behavior after mechanical stimulation (Fig. 3*E*). In contrast, 80% of imidacloprid-fed *dSlo2/K_{Na}^-* flies exhibited paralysis following mechanical stimulation (Fig. 3*E*). Together, our results using imidacloprid to overactivate nAChRs suggest that dSlo2/K_{Na} channels function to dampen this excessive activity and protect against detrimental developmental and behavioral consequences.

dSlo2 channels are activated by a TTX-sensitive Na^+ current in neurons

Mammalian Slo2/K_{Na} channels have been shown to be activated by Na^+ influx through TTX-sensitive Na^+ channels, and in particular, by the persistent current Na^+ current (I_{Nap}) that follows the transient Na^+ current component (Budelli et al., 2009; Hage and Salkoff, 2012). To test whether there is also a TTX-sensitive K^+ current present in *Drosophila* neurons, we assayed primary neurons dissociated from *ChAT-Gal4≫UAS-GFP* embryos, which express GFP in ChaT-positive neurons, and grown in culture for 9-10 DIV. In whole-cell perforated-patch mode, we applied voltage-clamp protocols to elicit voltage-dependent Na^+ and K^+ currents from ChAT-positive neurons. From a holding potential of −90 mV, we took 200 ms voltage jumps to potentials from −50 to 50 mV, in 10 mV increments. Based on extensive characterization of these neurons (Tsunoda and Salkoff, 1995a, b; Ping et al., 2011), this voltage protocol is expected to elicit a Na^+ current encoded by the single voltage-dependent Na^+ channel gene *para*, a rapidly activating transient A-type K^+ current encoded by the *K_v4/Shal* gene, and delayed-rectifier type K^+ currents encoded by the *K_v2/Shab* and *K_v3/Shaw* genes. In the first 100 ms of the voltage jump, Na^+ and K_v4/Shal channels are likely to be activated and carry currents in opposing directions, making the visualization of either incomplete. In the last 100 ms of the voltage jump, however, the transient Na^+ current component will be completely inactivated and only I_{Nap} and sustained K^+ currents will be represented. Thus, we measured the sustained current component, by averaging the last 60 ms, before and after TTX (1 μM) bath perfusion; any TTX-sensitive current was isolated by subtracting the whole-cell current after TTX application from the whole cell current before TTX application. We found a small outward current that could be measured from ~20 mV (Fig. 4*A*,*D*). The outward nature of this current suggests the presence of a TTX-sensitive K^+ current. To confirm that this TTX-sensitive K^+ current is Na^+-dependent, we also removed Na^+ from the extracellular bath solution and performed the same experimental protocol. Indeed, the small outward TTX-sensitive current was absent under these conditions (Fig. 4*B*,*E*).

We next tested whether this small sustained TTX-sensitive K^+ current was encoded by the *dSlo2/K_{Na}* gene. To do this, we recorded from ChAT-positive neurons in primary cultures made from the *dSlo2/K_{Na}^-* null mutant line. We found no outward TTX-sensitive current present in *dSlo2/K_{Na}^-* mutant neurons (Fig. 4*C*,*F*); instead, the TTX-sensitive current in *dSlo2/K_{Na}^-* mutant neurons was a small inward current that likely represents I_{Nap} (Fig. 4*F*). These results suggest that *dSlo2/K_{Na}* encodes a small sustained K^+ current in excitatory *Drosophila* neurons that is activated by Na^+ influx carried by TTX-sensitive Na^+ channels.

To examine whether dSlo2/K_{Na} channels are localized in close proximity to voltage-dependent Na^+ channels, we immunostained similarly cultured and aged primary neurons from a *Drosophila* line expressing endogenously labeled *dSlo2-myc* and *para-mCherry* (Ravenscroft et al., 2020). We found that dSlo2-myc and para-mCherry exhibited significant overlap in neuronal

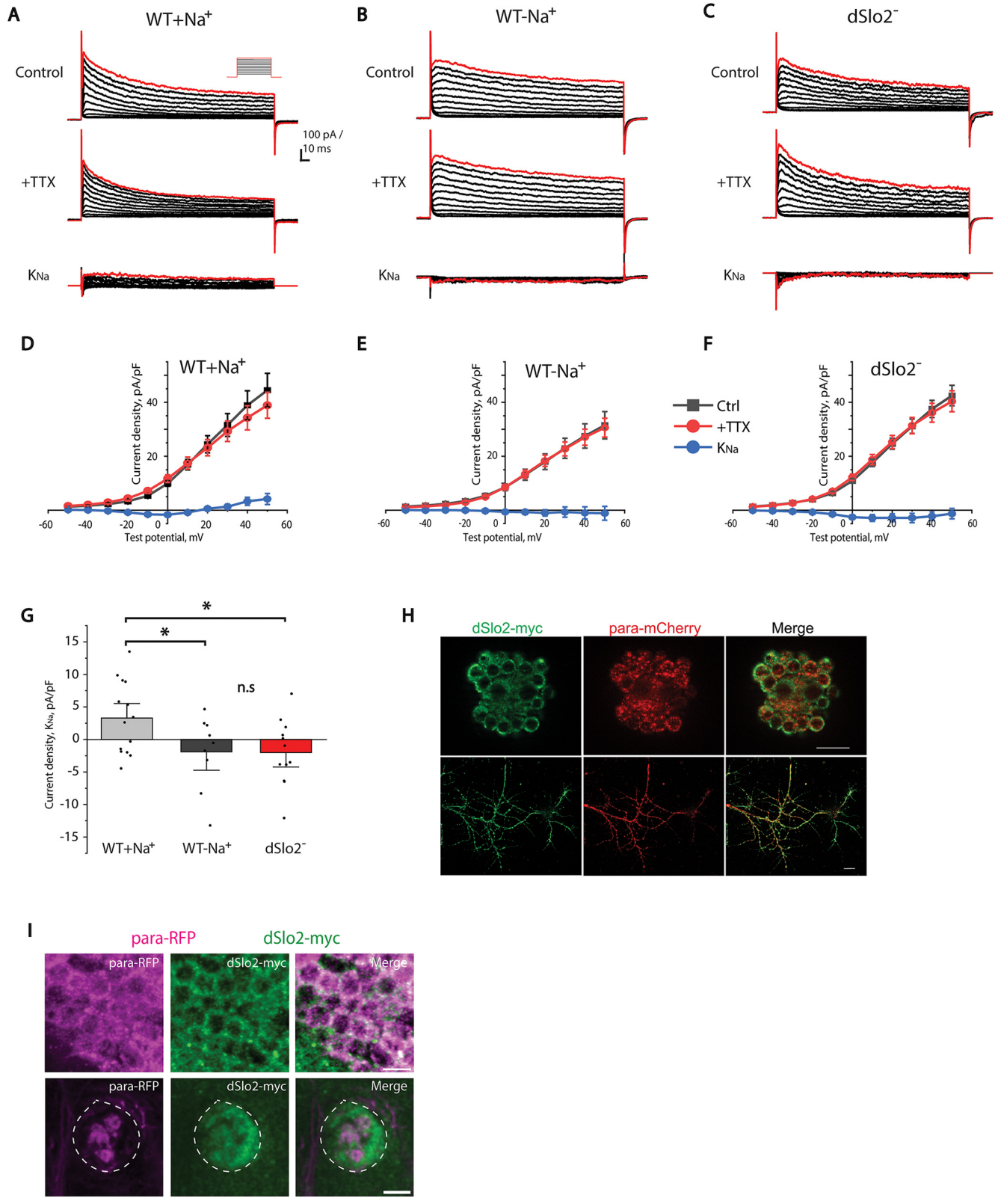

Figure 4. *dSlo2/K_{Na}* encodes a TTX-sensitive outward current in neurons. ***A-C***, Na^+ and K^+ currents elicited from representative WT neurons in Na^+-containing extracellular solution (***A***, WT+Na^+) or Na^+-free extracellular solution (***B***, WT-Na^+), and *dSlo2/K_{Na}^-* neurons in Na^+-containing extracellular solution (***C***, *dSlo2*$^-$) at 9 DIV in response to voltage jumps to −50 to 50 mV, in 10 mV increments, before (Control) and after 1 μM +TTX application. Current traces from the +TTX condition were subtracted from the Control condition to give TTX-sensitive current trace shown (K_{Na}). Calibration: 100 pA, 10 ms. ***D-F***, Plotted are current densities for Ctrl, +TTX, and K_{Na} currents, as described for ***A-C*** at indicated test potentials for WT+Na^+ (***D***), WT-Na^+ (***E***), and *dSlo2/K_{Na}^-* mutant (***F***) neurons. *n* = 12-14 cells. ***G***, Calculated current densities for the TTX-sensitive (K_{Na}) current in WT+Na^+, WT-Na^+, and *dSlo2*$^-$ mutant neurons at a test potential of 40 mV; *n* = 12-14 cells. ***D-G***, Data are mean ± SEM. *$p = 0.018$ (Student's *t* test). ***H***, Optical sections through a representative cluster of neuronal cell bodies (top) and extending processes (bottom) of primary neurons cultured (8-10 DIV) from *para-mCherry;dSlo2-myc* embryos. Cells are coimmunostained for dSlo2-myc (green) and para-mCherry (red). Scale bar, 10 μm. ***I***, Representative optical sections showing coimmunostaining of *para-RFP* (magenta) and *dSlo2-myc* (green) in KC somas (top; scale bar, 5 μm) and axons in the peduncle (bottom, dotted white outline; scale bar, 10 μm) from the intact adult brain.

cell bodies and processes at 8-10 DIV (Fig. 4*H*). In KCs of the adult brain, we observed that dSlo2-myc and para-RFP overlap in somas and in the peduncle, a structure housing axonal segments proximal to the KC cell body layer (Fig. 4*I*), but both were seemingly absent from more distal axonal regions in the mushroom body lobes. These results suggest that dSlo2/K_{Na} and voltage-dependent Na^+ channels often colocalize in similar neuronal subcompartments, where I_{Nap} influx through Na^+ channels could activate nearby dSlo2/K_{Na} channels.

dSlo2/KNa$^-$ mutant neurons exhibit excitability similar to WT neurons under basal conditions

We first examined whether *dSlo2/KNa*$^-$ null mutant neurons exhibit altered excitability under normal physiological conditions. In current-clamp mode, we ramped current injection from 0 to 150 pA over 1000 ms and recorded membrane voltage changes. We measured the charge transfer required to elicit the first action potential (AP) firing, the rate of change in membrane potential in the first 50 ms (slope), amplitude of the first AP, time to first AP peak, and the interval between the first and second APs. We found no differences between WT and *dSlo2/KNa*$^-$ mutants for all of these measurements (Fig. 5), with the exception of an increase in the interval between the first and second AP (Fig. 5*F*). Overall, however, there was no significant change in neuronal excitability under basal conditions. Membrane resistance, cell capacitance, and resting membrane potentials were also not different between WT and *dSlo2/KNa*$^-$ mutants (Table 1). These results are consistent with behavioral data in this study which show no difference between WT and *dSlo2/KNa*$^-$ mutants unless challenged with conditions of global overexcitation.

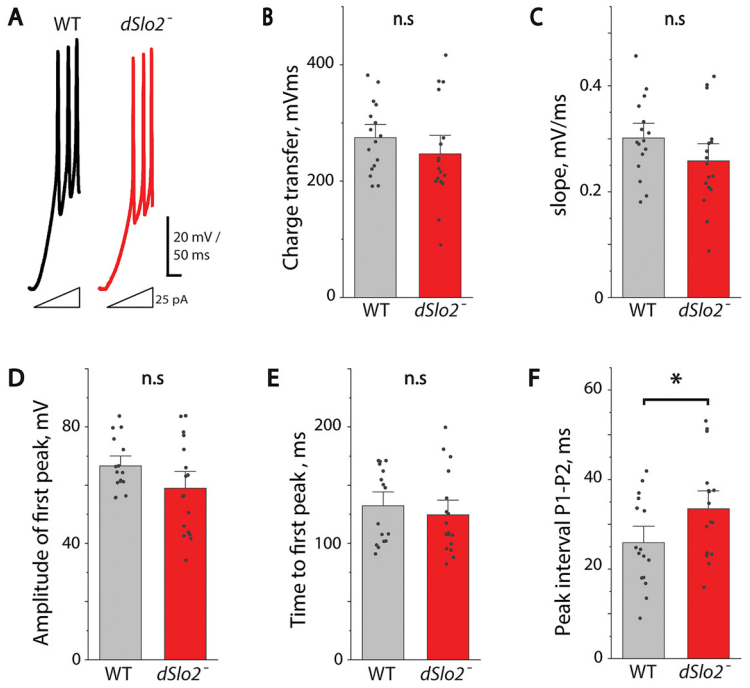

Figure 5. *dSlo2/KNa*$^-$ mutant neurons exhibit excitability similar to WT neurons under basal conditions. ***A***, Representative membrane voltage responses from WT and *dSlo2/KNa*$^-$ (*dSlo2*$^-$) neurons to ramped current injection from 0 to 150 pA over 1000 ms; the first 165 ms are shown. The following measurements were made: ***B***, charge transfer required to elicit the first AP; ***C***, rate of membrane potential change in the first 50 ms of ramp stimulation; ***D***, peak amplitude of the first AP; ***E***, time to the first AP peak; ***F***, interval between peaks of the first and second AP. $n = 17$ or 18 cells per genotype. Data are mean ± SEM. $^*p < 0.05$ (Student's *t* test).

Table 1. Passive electrical properties of WT and *dSlo2/K$_{Na}$*$^-$ neurons are similar

	Capacitance (pF)	Input resistance (GΩ)	Resting membrane potential (mV)
WT	8.17 ± 0.49 ($n = 17$)	4.27 ± 0.40 ($n = 39$)	−41.50 ± 2.39 ($n = 14$)
dSlo2$^-$	8.32 ± 0.90 ($n = 13$)	3.14 ± 0.52 ($n = 38$)	−40.10 ± 2.70 ($n = 23$)
p value, *t* test	0.89	0.09	0.70

Loss of *dSlo2/K$_{Na}$* in GEFS$^+$ seizure mutants exacerbate heat-induced seizure-like behavior

We next set out to test whether dSlo2/K_{Na} channels might dampen excitation under conditions of hyperexcitation created by elevated levels of I_{Nap}. In *Drosophila*, there are multiple seizure models that exhibit an enhanced I_{Nap} current. First, we examined the *GEFS*$^+$ mutant model. This model was designed to contain a genomic point mutation in the *para* Na^+ channel gene that is analogous to a human mutation that causes an elevated I_{Nap} current and underlies the disease, GEFS$^+$ (Abou-Khalil et al., 2001; Sun et al., 2012). Similar to effects in humans, *Drosophila GEFS*$^+$ mutants exhibit an enhanced I_{Nap} current and seizure-like activity in response to increased temperature (Sun et al., 2012) (Fig. 6*A*). In contrast, WT and *dSlo2/K$_{Na}$*$^-$ mutants did not induce any seizure-like activity at 40°C (Fig. 6*A*). We next examined whether the loss of dSlo2/K_{Na} channels in *GEFS*$^+$ mutants would affect seizure susceptibility. Since *GEFS*$^+$ mutants exhibit an enhanced I_{Nap} current, and I_{Nap} activates dSlo2/K_{Na} channels, we reasoned that dSlo2/K_{Na} channels might provide some initial protection against hyperactivity. If this hypothesis is correct, we expect that the loss of dSlo2/K_{Na} channels would result in greater seizure sensitivity. We compared the *GEFS*$^+$ mutation with and without the *dSlo2/K$_{Na}$*$^-$ null mutation. We found that, while 50% of *GEFS*$^+$ mutants exhibited seizure-like activity after ~100 s at 40°C, *GEFS*$^+$*; dSlo2/K$_{Na}$*$^-$ double mutants were significantly more sensitive to heat-induced seizure-like activity, with 50% of the flies seizing after only ~70 s (Fig. 6*A*). These results suggest that dSlo2/K_{Na} channels function to dampen hyperactivity and suppress seizure-like behavior.

Loss of *dSlo2/K$_{Na}$* in I_{Nap}-affected "bang-sensitive" seizure models results in increased susceptibility and prolonged seizure-like behavior

We next examined three "bang-sensitive" mutants that exhibit an elevated I_{Nap} current and consequent susceptibility to mechanically induced seizure-like activity. These mutants, *julius seizure*$^{iso7.8}$ (*jus*$^-$) (previously known as *slamdance*$^{iso7.8}$), *easily shocked*^{PC80}(*eas*$^-$), and *bang-senseless*^{1} (*bss*$^-$), have been well characterized as models of human epilepsy (Zhang et al., 2002; Song and Tanouye, 2008; Marley and Baines, 2011; Parker et al., 2011a, b). *jus*$^-$, *eas*$^-$, and *bss*$^-$ mutants all exhibit seizure-like activity induced by mechanical stress; this seizure-like activity has been well characterized both behaviorally and electrophysiologically (Benzer, 1971; Ganetzky and Wu, 1982; Pavlidis et al., 1994; Pavlidis and Tanouye, 1995; Kuebler et al., 2001; J. Lee and Wu, 2002; Song and Tanouye, 2008; Marley and Baines, 2011; Parker et al., 2011a). We set out to examine whether the *dSlo2/K$_{Na}$*$^-$ null mutation exacerbates these seizure-like phenotypes. Because homozygous *bss*$^-$ mutants have been reported to exhibit such a

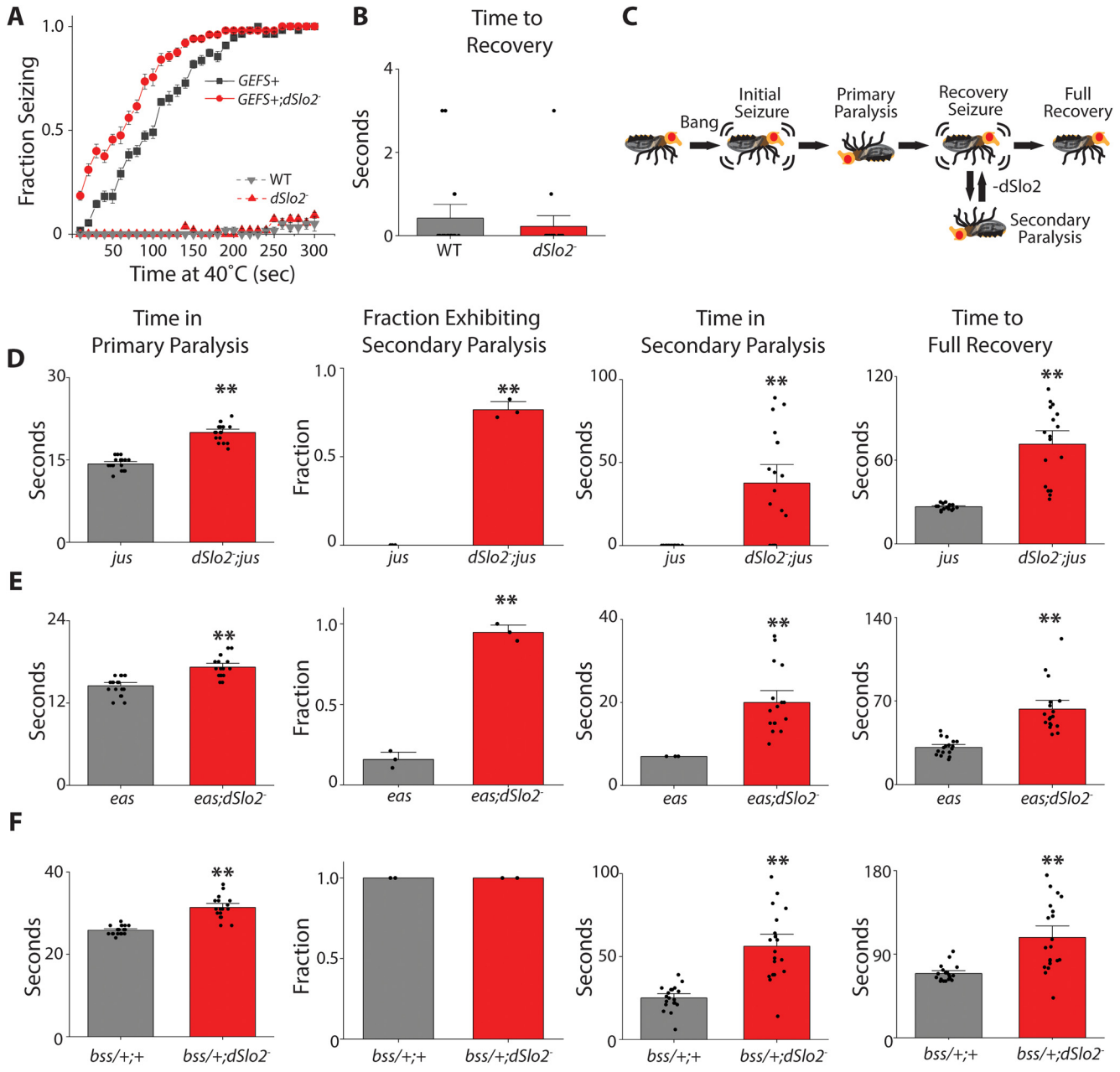

Figure 6. The absence of dSlo2/K_{Na} channels in multiple I_{Nap}-affected seizure models results in increased seizure susceptibility following heat/mechanical stimulation. ***A***, Mean fraction of flies exhibiting seizure-like behavior shown for WT, *dSlo2/K_{Na}^-*, *$GEFS^+$*, and *$GEFS^+$;dSlo2/K_{Na}^-* while subjected to 40°C for the times indicated. $n = 10$-12 groups of 5 individuals per genotype. ***B***, Time to full recovery following 10 s mechanical stimulation for WT and *dSlo2/K_{Na}^-* (*dSlo2*$^-$). ***C***, Diagram showing typical sequence of seizure behavior in "bang-sensitive" models following mechanical stimulation. ***D-F***, Mean time in primary paralysis, fraction of flies exhibiting secondary paralysis, time in secondary paralysis, and time to full recovery for individually assayed *jus*$^-$ (***D***), *eas*$^-$ (***E***), and *bss*$^{-/+}$ (***F***) mutants with and without the *dSlo2/K_{Na}^-* mutation, as indicated, immediately following 10 s mechanical stimulation. $n = 17$-19 flies per genotype. Data are mean ± SEM. Double mutants compared with *jus*$^-$, *eas*$^-$, and *bss*$^{-/+}$ backgrounds. $^{**}p < 0.01$ (Student's *t* test).

strong phenotype, it was not clear that we would be able to detect an exacerbated phenotype in this background; we therefore used *bss*$^{-/+}$ heterozygotes, which have been shown to exhibit a similar, albeit less severe, seizure-like phenotype (Kuebler and Tanouye, 2000; Parker et al., 2011b).

Mechanical stress was invoked by a 10 s vortex of single flies in empty vials. While WT and *dSlo2/K_{Na}^-* mutant flies immediately recovered from this mechanical stimulation (Fig. 6*B*), *eas*$^-$, and *bss*$^{-/+}$ mutants all exhibited the expected stereotypical sequence of seizure activity: a "primary paralysis" phase following an "initial seizure" that occurs during this mechanical stimulation, followed by a "recovery seizure," and finally, "full recovery" (as diagrammed in Fig. 6*C*; Fig. 6*D–F*), as previously reported (for review, see Parker et al., 2011a). Seizure-like activity was characterized by uncontrollable motor movement and an inability to stand or walk. We then tested whether and how the absence of *dSlo2/K_{Na}* affected this behavioral sequence in *jus*$^-$, *eas*$^-$, and *bss*$^{-/+}$ mutant backgrounds. We measured the time flies spent in primary paralysis, as well as the total time to full recovery. We found that the loss of dSlo2/K_{Na} channels in all bang-sensitive lines resulted in a significant increase in times of paralysis and times to full recovery (Fig. 6*D–F*). For example, seizure mutants' times to full recovery were lengthened by 57%-163% when combined with the *dSlo2/K_{Na}^-* mutation (Fig. 6*D–F*).

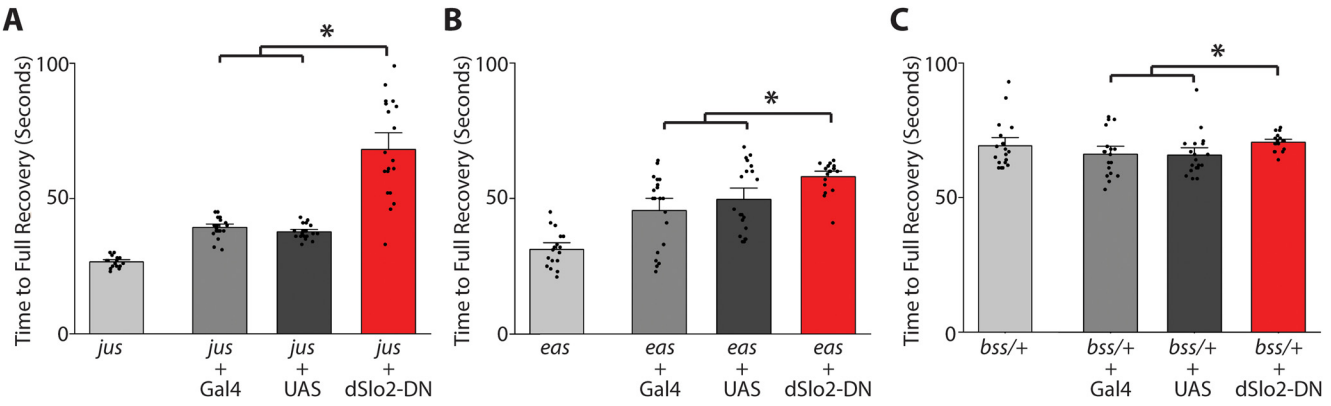

Figure 7. Expression of dominant-negative dSlo2/K_{Na} subunit (dSlo2/K_{Na}-DN) in cholinergic neurons prolongs induced seizure-like behavior in I_{Nap}-affected models. Shown are mean times that individual flies took to full recovery after mechanical stimulation. These times were measured in *jus*$^{-}$ (***A***), *eas*$^{-}$ (***B***), and *bss*$^{-/+}$ (***C***) mutants with *ChAT-Gal4* (Gal4), *UAS-dSlo2/K_{Na}-DN* (UAS), or *ChAT-Gal4≫UAS-dSlo2/K_{Na}-DN* (dSlo2-DN), as indicated. Data for *jus*$^{-}$, *eas*$^{-}$, and *bss*$^{-/+}$ alone are from Figure 6 and shown for comparison. Data are mean ± SEM. *$p < 0.05$ (Student's *t* test).

Interestingly, in *jus*$^{-}$ and *eas*$^{-}$ mutants, the absence of *dSlo2/K_{Na}* often caused a "secondary paralysis" period following the recovery seizure (diagrammed in Fig. 6*C*; Fig. 6*D–F*); this tendency was largely absent in the *jus*$^{-}$ and *eas*$^{-}$ mutant backgrounds alone, although routinely observed in *bss*$^{-/+}$ mutants (Fig. 6*D–F*). We quantified the duration of these secondary paralysis periods and found that the loss of *dSlo2/K_{Na}* also prolonged these periods in all mutant backgrounds (Fig. 6*D–F*).

We then tested whether dSlo2/K_{Na} channels play this protective role in excitatory neurons of the CNS, as suggested by our expression studies (Fig. 2*A*). To do this, we generated a transgenic line expressing a dominant-negative (DN) *dSlo2/K_{Na}* subunit under the control of *UAS* (*UAS-dSlo2/K_{Na}-DN*). In this *dSlo2/K_{Na}-DN* sequence, the highly conserved K^+ channel pore sequence, glycine-tyrosine-glycine (GYG), was mutated to three alanines (GYG>AAA); this mutation has previously been shown to produce subunits that, when multimerized with WT subunits, renders K^+ channels nonfunctional (Perozo et al., 1993; Barry et al., 1998; Abou Tayoun et al., 2011; Ping et al., 2011). Because we had observed widespread expression of dSlo2/K_{Na} in most cholinergic neurons throughout the adult brain, we used *ChAT-Gal4* to drive expression of *UAS-dSlo2/K_{Na}-DN* in cholinergic neurons of *jus*$^{-}$, *eas*$^{-}$, and *bss*$^{-/+}$ mutant lines. We found that *ChAT-Gal4≫UAS-dSlo2/K_{Na}-DN* expression increased the time from mechanical stimulation to full recovery in each of these seizure lines (Fig. 7). Together, our results suggest that dSlo2/K_{Na} channels protect excitatory neurons from hyperactivity and aid in the prevention of induced seizure-like behavior.

dSlo2/K_{Na} channels protect flies from mechanically induced seizure-like behavior primed by pharmacological enhancement of I_{Nap}

We next tested whether pharmacological enhancement of the I_{Nap} current component would also prime the nervous system for induction of seizure-like behavior, and whether the loss of *dSlo2/K_{Na}* would exacerbate this behavior. To do this, we considered veratridine, which has been shown in multiple mammalian cell types to prolong the open state of Na^+ channels, thereby increasing the I_{Nap} current (Barnes and Hille, 1988; Hage and Salkoff, 2012). We tested veratridine in primary cultured *Drosophila* neurons and found that bath perfusion of veratridine (5 μM) indeed increased the I_{Nap} current component of the Na^+ current, with no significant effect on the transient Na^+ current component (Fig. 8*A*).

We then fed flies either vehicle (mock-treated) or veratridine (20 μM) for 2 h and subjected them to mechanical stress with a 10 s vortex. While this mechanical stress did not induce the stereotypical sequence of seizure-like behavior exhibited by bang-sensitive flies (Fig. 6*C*), it did result in seizure-like behavior immediately following mechanical stimulation. To test whether dSlo2/K_{Na} channels function protectively against this seizure-like behavior, we compared mock- or veratridine-fed WT and *dSlo2/K_{Na}*$^{-}$ flies. We found that a significantly higher fraction of veratridine-fed *dSlo2/K_{Na}*$^{-}$ mutants displayed mechanically induced seizure-like behavior, compared with mock-fed *dSlo2/K_{Na}*$^{-}$ mutants or veratridine-fed WT flies (Fig. 8*B*). To test the specificity of this effect, we also mock- and veratridine-fed null mutants of the small-conductance Ca^{2+}-activated K^+ channel gene (*SK*$^{-}$) and the voltage-dependent K_v1/*Shaker* K^+ channel gene (*Sh*^{KS133}). *SK*$^{-}$ and *Sh*^{KS133} mutants, whether mock- or veratridine-fed, did not exhibit any more seizure-like behavior than WT (Fig. 8*B*). Our results suggest that dSlo2/K_{Na} channels protect neurons from seizure induction also in this veratridine-primed model, in which the system is confronted with a global increase in I_{Nap}.

The loss of *dSlo2/K_{Na}* reveals a spontaneous seizure phenotype in I_{NaP}-affected seizure models

Bang-sensitive mutants are well known to require mechanical stress to induce seizure-like behavior, and this was largely true for our veratridine-primed model. However, we noticed that, when these seizure models contained the *dSlo2/K_{Na}*$^{-}$ mutation, a significant number of flies appeared to exhibit spontaneous seizure-like behavior. One possibility is that dSlo2/K_{Na} channels contribute to the threshold for seizure induction, and when absent in these seizure models, threshold is significantly reduced, thereby enabling spontaneous seizures to occur. To test this, we quantified the number of seizures observed in groups of 10 flies over a 15 min period; we first tested *jus*$^{-}$, *eas*$^{-}$, and *bss*$^{-/+}$ mutants with and without *dSlo2/K_{Na}*. As expected, *jus*$^{-}$, *eas*$^{-}$, and *bss*$^{-/+}$ flies all exhibited little to no spontaneous seizure-like activity, similar to WT (Fig. 9*A*). In contrast, *dSlo2/K_{Na}*$^{-}$*; jus*$^{-}$ and *bss*$^{-/+}$*; dSlo2/K_{Na}*$^{-}$ double mutants both displayed a significant number of spontaneous seizures (Fig. 9*A*); *dSlo2/K_{Na}*$^{-}$*;eas*$^{-}$ double mutants, however, were similar to WT (Fig. 9*A*), and it is unclear why the *eas*$^{-}$ mutant background was less susceptible to spontaneous seizures

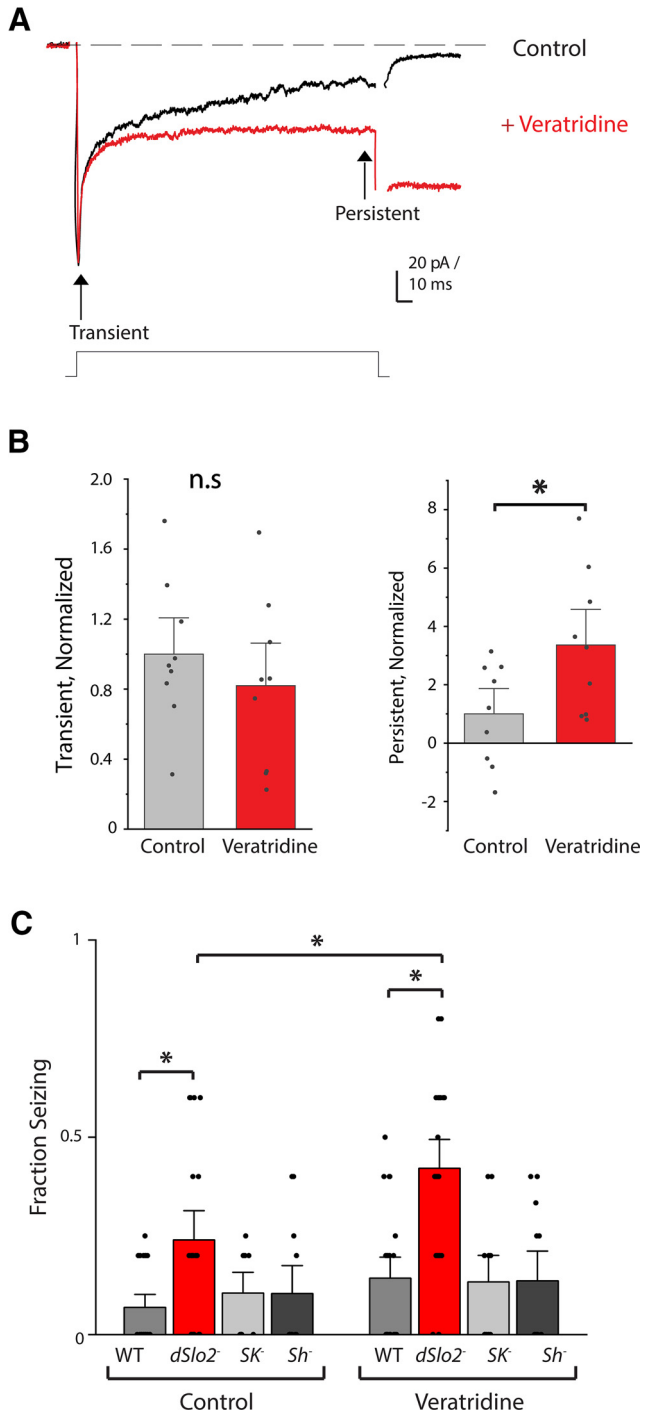

Figure 8. *dSlo2/K_{Na}^-* mutants fed veratridine, an enhancer of I_{Nap}, exhibit increased susceptibility to mechanically induced seizure-like behavior. ***A***, Representative whole-cell Na^+ current recorded from a WT neuron (9 DIV) from a holding potential of −90 mV to a test potential of −20 mV before (Control; black trace) and after 5 μm veratridine (+veratridine; red trace) application. Transient and persistent components of the Na^+ current are indicated. Calibration: 20 pA, 10 ms. ***B***, Normalized Na^+ current densities for the transient current component (left; transient) and persistent I_{Nap} current component (right; persistent) from Control and veratridine-treated neurons. $n = 9$ cells. ***C***, The mean fraction of flies exhibiting seizure-like behavior immediately following a 10 s mechanical stimulation. WT, *dSlo2/K_{Na}^-*, *SK*, and *Sh^{KS133}* (*Sh*) flies were fed either vehicle (0.05% DMSO, Mock) or 20 μM veratridine (Vtd) for 2 h before mechanical stimulation. $n = 10$-23 groups of 5 flies/vial. Data are mean ± SEM. *$p < 0.05$ (Student's *t* test).

than the other mutants. *dSlo2/K_{Na}^-* mutants themselves displayed minimal spontaneous seizure activity (Fig. 9*A*), suggesting that conditions for spontaneous seizure-activity is primed by an enhancement in I_{Nap}, and revealed by a lack of dSlo2/K_{Na} channels. To test whether this effect is specific to the loss of dSlo2/K_{Na} channels in cholinergic neurons, we drove expression of the dominant-negative *UAS-dSlo2/K_{Na}-DN* transgene exclusively in cholinergic neurons in the *jus*$^-$ mutant, and assayed for spontaneous seizure-like activity. Similar to the *dSlo2/K_{Na}^-;jus*$^-$ double mutant, *ChAT-Gal4≫UAS-dSlo2/K_{Na}-DN;jus*$^-$ flies exhibited a significantly increased number of spontaneous seizures, compared with cholinergic expression of *dSlo2-DN* alone, or the *jus* mutation combined with the *ChAT-Gal4* or *UAS-dSlo2/K_{Na}-DN* alone (Fig. 9*B*).

We also tested whether veratridine-enhancement of I_{Nap} would similarly induce spontaneous seizure-like activity that would be exposed with the lack of dSlo2/K_{Na} channels. WT and *dSlo2/K_{Na}^-* flies, as well as *SK*$^-$ and *Sh^{KS133}* K^+ channel mutants, were mock- or veratridine-fed for 2 h. Then, groups of 10 were observed over a 15 min period for any seizure-like activity. We found that the number of seizures was very low and not significantly different in WT, *SK*$^-$, and *Sh^{KS133}* flies, whether mock- or veratridine-fed (Fig. 9*C*). In contrast, veratridine-fed *dSlo2/K_{Na}^-* mutants exhibited a significantly elevated number of spontaneous seizures compared with veratridine-fed WT flies or *dSlo2/K_{Na}^-* mock-fed flies (Fig. 9*C*). We also examined whether there were differences in the duration of observed seizures. *dSlo2/K_{Na}^-;jus*$^-$ and *bss*$^{-/+}$*;dSlo2/K_{Na}^-* double mutants exhibited a wider distribution of seizure durations than single mutant lines (Fig. 9*D*, *E*). Similarly, veratridine-fed *dSlo2/K_{Na}^-* mutants displayed a wider range of seizure durations compared with veratridine-fed WT flies (Fig. 9*F*); all seizure-like events observed in WT flies lasted <3 s, while seizure events in *dSlo2/K_{Na}^-* mutants lasted from 0.7 to 89 s. Because of the low numbers of seizures seen in control lines, however, we were not able to perform meaningful statistical analyses on these distributions. Together, our results suggest that, when dSlo2/K_{Na} channels are absent in models already susceptible to seizure, seizure thresholds are lowered, resulting in an increased incidence of induced as well as spontaneous seizure behavior.

Discussion

In this study, we show that, when dSlo2/K_{Na} channels are absent in genetic and pharmacological models that increase Na^+ influx carried by either nAChRs or voltage-gated Na^+ channels, effects such as seizure-like behavior, paralysis, and death, are even worse, suggesting that a role of dSlo2/K_{Na} channels is to help prevent these outcomes when the nervous system is overexcited. In particular, our data suggest that dSlo2/K_{Na} channels in *Drosophila*, like their mammalian counterparts, are activated by the I_{Nap} current carried by voltage-dependent Na^+ channels. We examined four genetic seizure models and a newly introduced pharmacological (veratridine) model with enhanced I_{Nap} currents. The mechanism underlying the enhanced I_{Nap} in each of these genetic seizure mutants, however, is different. *jus*$^-$ and *eas*$^-$ mutations affect a novel transmembrane protein of unknown function (Horne et al., 2017) and ethanolamine kinase (Pavlidis et al., 1994), respectively, which have each been reported to affect alternative splicing of the *para* Na^+ channel gene, increasing the inclusion of "exon-L," which has been shown to be associated with increased I_{Nap} (Lin et al., 2012). In contrast, the increase in I_{Nap} in the *bss*$^-$ and *GEFS*$^+$ lines are because of point mutations

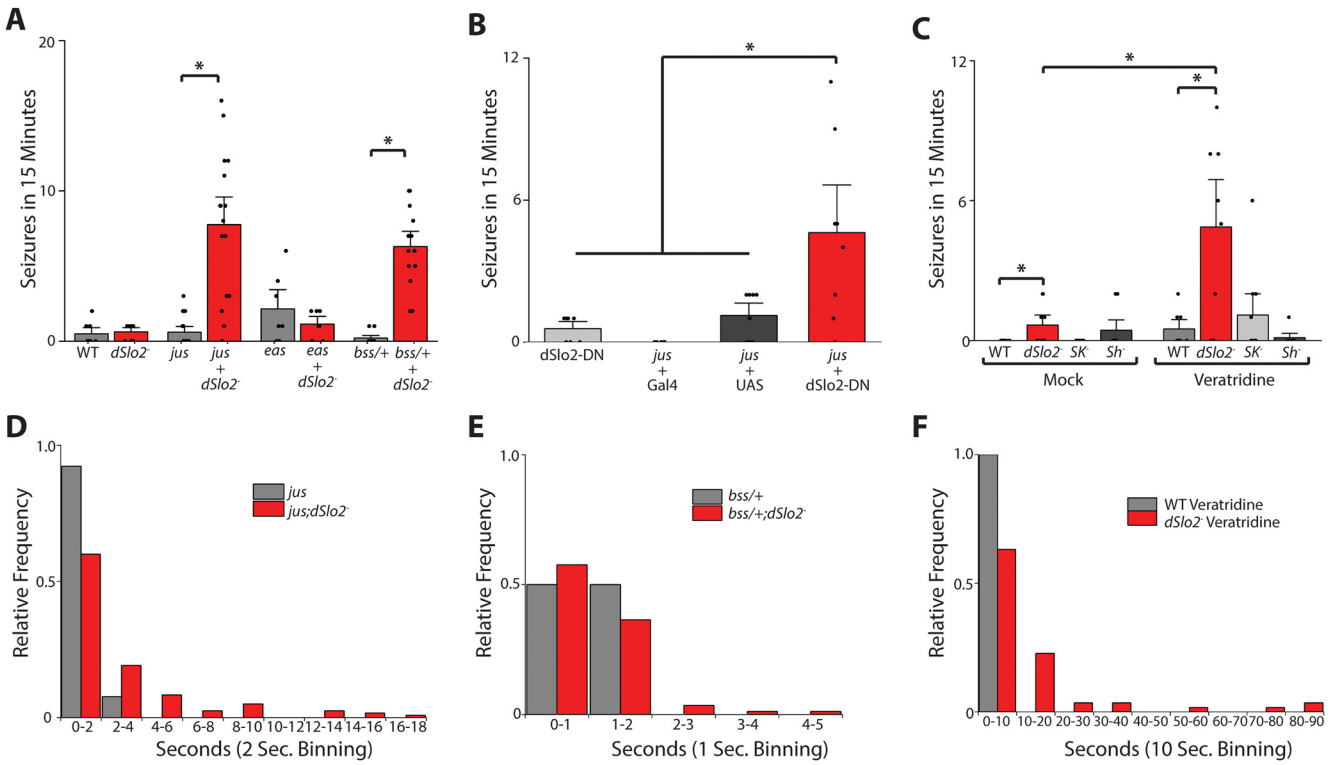

Figure 9. Absence of dSlo2/K_{Na} channels in multiple I_{Nap}-affected seizure models results in an increased incidence of spontaneous seizures. ***A-C***, Data are mean numbers of spontaneous seizures observed in groups of 10 flies over a 15 min period of time. ***A***, Mean numbers of spontaneous seizures for WT, *dSlo2/K_{Na}^-*, and *jus*$^-$, *eas*$^-$, *bss*$^{-/+}$ mutations alone and in combination with *dSlo2/K_{Na}^-*, as indicated. $n = 7$ or 8 groups for WT and single mutants; $n = 14$-16 groups for double-mutant genotypes with *dSlo2*$^-$. ***B***, Mean numbers of spontaneous seizures for *ChAT-Gal4≫UAS-dSlo2/K_{Na}-DN* (dSlo2-DN), and *jus*$^-$ alone or in combination with *ChAT-Gal4* (Gal4), *UAS-dSlo2/K_{Na}-DN* (UAS), or dSlo2-DN, as indicated. $n = 7$ or 8 groups per genotype. ***C***, Mean numbers of spontaneous seizures for WT, *dSlo2/K_{Na}^-*, *SK*$^-$, and *Sh*^{KS133} (*Sh*$^-$) flies fed either vehicle (0.05% DMSO, Mock) or 20 μM veratridine for 2 h before assay. $n = 8$-10 groups per genotype. Data are mean ± SEM. *$p < 0.05$ (Student's *t* test). ***D-F***, Shown, for descriptive purposes, are histograms of durations of spontaneous seizures grouped into indicated bins for indicated genotypes and conditions.

in the *para* gene itself (Parker et al., 2011b; Sun et al., 2012). Notably, mutations that increase I_{Nap} in mammalian systems have been associated with multiple types of human epilepsy (Kearney et al., 2001; Lossin et al., 2002; Vanoye et al., 2006; Chen et al., 2011). And in all four genetic seizure models and veratridine-fed WT flies, we showed that the loss of dSlo2/K_{Na} channels results in increased seizure susceptibility and severity. The observation that the loss of dSlo2/K_{Na} channels similarly affects multiple I_{Nap}-affected *Drosophila* models bolsters the suggestion that the protective role of dSlo2/K_{Na} channels is indeed because of activation by the enhanced I_{Nap} current.

Interestingly, the degree to which the *dSlo2/K_{Na}^-* null mutation and *dSlo2/K_{Na}-DN* dominant-negative transgene exacerbated seizure phenotypes of the bang-sensitive mutants, *jus*$^-$, *eas*$^-$, and *bss*$^-$, seems to be inversely related to the reported severity of each mutant phenotype. For example, the *jus*$^-$ mutant has been reported to exhibit the least severe phenotype of the three bang-sensitive mutants we tested (Kuebler and Tanouye, 2000), yet it was in this background that *dSlo2/K_{Na}^-* and *dSlo2/K_{Na}-DN* resulted in the greatest percent increase in seizure indicators (e.g., times of paralysis, times to full recovery, frequency of seizures, etc.) in both induced and spontaneous seizure-like behavior. In contrast, we saw the mildest changes in seizure indicators with the *bss*$^-$ mutant, which has been reported to have the lowest seizure-threshold and most severe seizure phenotype of the bang-sensitive mutants (Kuebler and Tanouye, 2000). The reason for this trend is unclear, but one speculation is that dSlo2/K_{Na} channels may function protectively as a first line of defense that raises the threshold for seizure induction, but as sustained and more severe overexcitation persists, dSlo2/K_{Na} channels can do little to alleviate ensuing seizure activity. This is a point that may need to be considered when evaluating conditions under which Slo2/K_{Na} channels contribute to seizure threshold in mammalian systems. Little has been reported about the role of Slo2/K_{Na} channels in seizure; in a recent report, the KO of *Slo2.2/Slack/K_{Na}1.1* has been shown to result in a decrease in the electric shock stimulus needed to induce a seizure in a hindlimb extension assay (Quraishi et al., 2020).

Although roles for Slo2/K_{Na} channels have been identified in nociceptive, thermal, and mechanical sensation (R. Lu et al., 2015; Martinez-Espinosa et al., 2015; Evely et al., 2017; Tomasello et al., 2017), as well as in reversal and motor learning (Bausch et al., 2015; Quraishi et al., 2020), there is a clear link between Slo2/K_{Na} channels and nonphysiological hyperactivity. For example, there are numerous mutations in human *Slo2/K_{Na} KCNT1/KCNT2* genes, which have been associated with multiple forms of epilepsy, including malignant migrating partial seizures of infancy (MMPSI), autosomal dominant nocturnal frontal lobe epilepsy (ADNFLE), Ohtahara syndrome, sudden unexplained death in epilepsy (SUDEP), multifocal epilepsy, leukoencephalopathy, Brugada syndrome, and epilepsy of infancy with migrating focal seizures (EIMFS) (Heron et al., 2012; Ishii et al., 2013; Møller et al., 2015; Gururaj et al., 2017; Ambrosino et al., 2018; Mao et al., 2020). Some of these human mutations have been recapitulated in *Xenopus* oocytes (Barcia et al., 2012; Kim et al., 2014; Milligan et al., 2014; Tang et al., 2016; McTague et al., 2018), CHO cells (Rizzo et al., 2016; Mao et al., 2020), HEK cells (Ambrosino et al., 2018), as well as human iPSC-derived neurons

(Quraishi et al., 2019), revealing both loss- and gain-of-function mutations. An enduring question in the field has been as follows: how do the many gain-of-function K_{Na} channel mutations lead to hyperactivity? Genetically tractable systems, such as *Drosophila*, may provide *in vivo* modeling to eventually address this question.

Multiple factors contribute to the complexity of how Slo2/K_{Na} channels affect neuronal excitability. For example, we found that the subcellular distribution of dSlo2/K_{Na} channels varied from one cell type to another, suggesting that dSlo2/K_{Na} channels likely affect excitability differently, depending on cell type. In addition, various factors, including Cl^- and NAD^+, have been reported to regulate Na^+ sensitivity of Slo2/K_{Na} channels (Yuan et al., 2000, 2003 Bhattacharjee et al., 2003;; Tamsett et al., 2009). Slo2/K_{Na} activation has also been reported downstream of multiple sources of Na^+, including glutamate receptors, H-channels, and cyclic nucleotide gated channels (Nanou and El Manira, 2007; S. Lu et al., 2010; Aoki et al., 2018); little, however, is known about the physical interaction/proximity of Slo2/K_{Na} channels to these channels or Na^+ channels, which would greatly influence the responsiveness and role of Slo2/K_{Na} channels. Finally, we found that enhancement of seizure indicators by the *dSlo2/K_{Na}^-* mutation in seizure prone backgrounds was difficult to rescue with exogenous expression of *dSlo2/K_{Na}* (data not shown); one speculation is that neurons are very sensitive to expressed levels of *dSlo2/K_{Na}*, making it difficult to titrate the right amount of *dSlo2/K_{Na}* expression to rescue the *dSlo2/K_{Na}^-* mutant phenotype without overexpressing *dSlo2/K_{Na}* above WT levels. Regulating precise expression levels of *dSlo2/K_{Na} in vivo* may be an additional challenge important to understanding how dSlo2/K_{Na} channels affect neuronal excitability.

Our current study supports a model in which one role of dSlo2/K_{Na} channels is to provide a reserve K^+ conductance that suppresses seizure induction when the nervous system is confronted with excessive excitation. It will be interesting for future studies to explore what factors distinguish this protective role of dSlo2/K_{Na} channels from roles in sensory processing and learning/memory function.

References

Abou-Khalil B, Ge Q, Desai R, Ryther R, Bazyk A, Bailey R, Haines JL, Sutcliffe JS, George AL Jr (2001) Partial and generalized epilepsy with febrile seizures plus and a novel SCN1A mutation. Neurology 57:2265–2272.

Abou Tayoun AN, Li X, Chu B, Hardie RC, Juusola M, Dolph PJ (2011) The *Drosophila* SK channel (dSK) contributes to photoreceptor performance by mediating sensitivity control at the first visual network. J Neurosci 31:13897–13910.

Akaike N, Shirasaki T, Yakushiji T (1991) Quinolones and fenbufen interact with GABAA receptor in dissociated hippocampal cells of rat. J Neurophysiol 66:497–504.

Ambrosino P, Soldovieri MV, Bast T, Turnpenny PD, Uhrig S, Biskup S, Docker M, Fleck T, Mosca I, Manocchio L, Iraci N, Taglialatela M, Lemke JR (2018) De novo gain-of-function variants in KCNT2 as a novel cause of developmental and epileptic encephalopathy. Ann Neurol 83:1198–1204.

Aoki I, Tateyama M, Shimomura T, Ihara K, Kubo Y, Nakano S, Mori I (2018) SLO potassium channels antagonize premature decision making in *C. elegans*. Commun Biol 1:123.

Barcia G, Fleming MR, Deligniere A, Gazula VR, Brown MR, Langouet M, Chen H, Kronengold J, Abhyankar A, Cilio R, Nitschke P, Kaminska A, Boddaert N, Casanova JL, Desguerre I, Munnich A, Dulac O, Kaczmarek LK, Colleaux L, Nabbout R (2012) De novo gain-of-function KCNT1 channel mutations cause malignant migrating partial seizures of infancy. Nat Genet 44:1255–1259.

Barnes S, Hille B (1988) Veratridine modifies open sodium channels. J Gen Physiol 91:421–443.

Barry DM, Xu H, Schuessler RB, Nerbonne JM (1998) Functional knockout of the transient outward current, long-QT syndrome, and cardiac remodeling in mice expressing a dominant-negative Kv4 alpha subunit. Circ Res 83:560–567.

Bausch AE, Dieter R, Nann Y, Hausmann M, Meyerdierks N, Kaczmarek LK, Ruth P, Lukowski R (2015) The sodium-activated potassium channel Slack is required for optimal cognitive flexibility in mice. Learn Mem 22:323–335.

Benzer S (1971) From the gene to behavior. JAMA 218:1015–1022.

Bhattacharjee A, Gan L, Kaczmarek LK (2002) Localization of the Slack potassium channel in the rat central nervous system. J Comp Neurol 454:241–254.

Bhattacharjee A, Joiner WJ, Wu M, Yang Y, Sigworth FJ, Kaczmarek LK (2003) Slick (Slo2.1), a rapidly-gating sodium-activated potassium channel inhibited by ATP. J Neurosci 23:11681–11691.

Bhattacharjee A, von Hehn CA, Mei X, Kaczmarek LK (2005) Localization of the Na^+-activated K^+ channel Slick in the rat central nervous system. J Comp Neurol 484:80–92.

Brown JT, Chin J, Leiser SC, Pangalos MN, Randall AD (2011) Altered intrinsic neuronal excitability and reduced Na^+ currents in a mouse model of Alzheimer's disease. Neurobiol Aging 32:2109.e1-e14.

Brown LA, Ihara M, Buckingham SD, Matsuda K, Sattelle DB (2006) Neonicotinoid insecticides display partial and super agonist actions on native insect nicotinic acetylcholine receptors. J Neurochem 99:608–615.

Brown MR, Kronengold J, Gazula VR, Spilianakis CG, Flavell RA, von Hehn CA, Bhattacharjee A, Kaczmarek LK (2008) Amino-termini isoforms of the Slack K^+ channel, regulated by alternative promoters, differentially modulate rhythmic firing and adaptation. J Physiol 586:5161–5179.

Budelli G, Hage TA, Wei A, Rojas P, Jong YJ, O'Malley K, Salkoff L (2009) Na^+-activated K^+ channels express a large delayed outward current in neurons during normal physiology. Nat Neurosci 12:745–750.

Busche MA, Eichhoff G, Adelsberger H, Abramowski D, Wiederhold KH, Haass C, Staufenbiel M, Konnerth A, Garaschuk O (2008) Clusters of hyperactive neurons near amyloid plaques in a mouse model of Alzheimer's disease. Science 321:1686–1689.

Busche MA, Chen X, Henning HA, Reichwald J, Staufenbiel M, Sakmann B, Konnerth A (2012) Critical role of soluble amyloid-beta for early hippocampal hyperactivity in a mouse model of Alzheimer's disease. Proc Natl Acad Sci USA 109:8740–8745.

Calvo M, Davies AJ, Hebert HL, Weir GA, Chesler EJ, Finnerup NB, Levitt RC, Smith BH, Neely GG, Costigan M, Bennett DL (2019) The genetics of neuropathic pain from model organisms to clinical application. Neuron 104:637–653.

Chen S, Su H, Yue C, Remy S, Royeck M, Sochivko D, Opitz T, Beck H, Yaari Y (2011) An increase in persistent sodium current contributes to intrinsic neuronal bursting after status epilepticus. J Neurophysiol 105:117–129.

Choi DW (2020) Excitotoxicity: still hammering the ischemic brain in 2020. Front Neurosci 14:579953.

Davis KE, Fox S, Gigg J (2014) Increased hippocampal excitability in the 3xTgAD mouse model for Alzheimer's disease in vivo. PLoS One 9: e91203.

Denecke S, Fusetto R, Batterham P (2017a) Describing the role of *Drosophila melanogaster* ABC transporters in insecticide biology using CRISPR-Cas9 knockouts. Insect Biochem Mol Biol 91:1–9.

Denecke S, Fusetto R, Martelli F, Giang A, Battlay P, Fournier-Level A, O' Hair RA, Batterham P (2017b) Multiple P450s and variation in neuronal genes underpins the response to the insecticide imidacloprid in a population of *Drosophila melanogaster*. Sci Rep 7:11338.

Deng PY, Klyachko VA (2021) Channelopathies in fragile X syndrome. Nat Rev Neurosci 22:275–289.

Diao F, White BH (2012) A novel approach for directing transgene expression in *Drosophila*: t 2A-Gal4 in-frame fusion. Genetics 190:1139–1144.

Diao F, Ironfield H, Luan H, Diao F, Shropshire WC, Ewer J, Marr E, Potter CJ, Landgraf M, White BH (2015) Plug-and-play genetic access to drosophila cell types using exchangeable exon cassettes. Cell Rep 10:1410–1421.

Dryer SE (1994) Na(+)-activated K^+ channels: a new family of large-conductance ion channels. Trends Neurosci 17:155–160.

Eadaim A, Hahm ET, Justice ED, Tsunoda S (2020) Cholinergic synaptic homeostasis is tuned by an NFAT-mediated alpha7 nAChR-Kv4/Shal coupled regulatory system. Cell Rep 32:108119.

Evely KM, Pryce KD, Bausch AE, Lukowski R, Ruth P, Haj-Dahmane S, Bhattacharjee A (2017) Slack KNa channels influence dorsal horn synapses and nociceptive behavior. Mol Pain 13:1744806917714342.

Fisher RS, van Emde Boas W, Blume W, Elger C, Genton P, Lee P, Engel J Jr (2005) Epileptic seizures and epilepsy: definitions proposed by the International League Against Epilepsy (ILAE) and the International Bureau for Epilepsy (IBE). Epilepsia 46:470–472.

Ganetzky B, Wu CF (1982) Indirect suppression involving behavioral mutants with altered nerve excitability in *Drosophila melanogaster*. Genetics 100:597–614.

Gibson JR, Bartley AF, Hays SA, Huber KM (2008) Imbalance of neocortical excitation and inhibition and altered UP states reflect network hyperexcitability in the mouse model of fragile X syndrome. J Neurophysiol 100:2615–2626.

Gratz SJ, Harrison MM, Wildonger J, O'Connor-Giles KM (2015a) Precise genome editing of *Drosophila* with CRISPR RNA-guided Cas9. Methods Mol Biol 1311:335–348.

Gratz SJ, Rubinstein CD, Harrison MM, Wildonger J, O'Connor-Giles KM (2015b) CRISPR-Cas9 genome editing in *Drosophila*. Curr Protoc Mol Biol 111:31.2.1–31.2.20.

Gunes ZI, Kan VW, Ye X, Liebscher S (2020) Exciting complexity: the role of motor circuit elements in ALS pathophysiology. Front Neurosci 14:573.

Gururaj S, Palmer EE, Sheehan GD, Kandula T, Macintosh R, Ying K, Morris P, Tao J, Dias KR, Zhu Y, Dinger ME, Cowley MJ, Kirk EP, Roscioli T, Sachdev R, Duffey ME, Bye A, Bhattacharjee A (2017) A de novo mutation in the sodium-activated potassium channel KCNT2 alters ion selectivity and causes epileptic encephalopathy. Cell Rep 21:926–933.

Hage TA, Salkoff L (2012) Sodium-activated potassium channels are functionally coupled to persistent sodium currents. J Neurosci 32:2714–2721.

Hahm ET, Nagaraja RY, Waro G, Tsunoda S (2018) Cholinergic homeostatic synaptic plasticity drives the progression of Abeta-induced changes in neural activity. Cell Rep 24:342–354.

Hartley DM, Walsh DM, Ye CP, Diehl T, Vasquez S, Vassilev PM, Teplow DB, Selkoe DJ (1999) Protofibrillar intermediates of amyloid beta-protein induce acute electrophysiological changes and progressive neurotoxicity in cortical neurons. J Neurosci 19:8876–8884.

Heisenberg M, Borst A, Wagner S, Byers D (1985) *Drosophila* mushroom body mutants are deficient in olfactory learning. J Neurogenet 2:1–30.

Heron SE, Smith KR, Bahlo M, Nobili L, Kahana E, Licchetta L, Oliver KL, Mazarib A, Afawi Z, Korczyn A, Plazzi G, Petrou S, Berkovic SF, Scheffer IE, Dibbens LM (2012) Missense mutations in the sodium-gated potassium channel gene KCNT1 cause severe autosomal dominant nocturnal frontal lobe epilepsy. Nat Genet 44:1188–1190.

Horne M, Krebushevski K, Wells A, Tunio N, Jarvis C, Francisco G, Geiss J, Recknagel A, Deitcher DL (2017) *julius seizure*, a *Drosophila* mutant, defines a neuronal population underlying epileptogenesis. Genetics 205:1261–1269.

Huang F, Wang X, Ostertag EM, Nuwal T, Huang B, Jan YN, Basbaum AI, Jan LY (2013) TMEM16C facilitates Na(+)-activated K^+ currents in rat sensory neurons and regulates pain processing. Nat Neurosci 16:1284–1290.

Huttunen JK, Airaksinen AM, Barba C, Colicchio G, Niskanen JP, Shatillo A, Sierra Lopez A, Ndode-Ekane XE, Pitkänen A, Gröhn OH (2018) Detection of hyperexcitability by functional magnetic resonance imaging after experimental traumatic brain injury. J Neurotrauma 35:2708–2717.

Ihara M, Hikida M, Matsushita H, Yamanaka K, Kishimoto Y, Kubo K, Watanabe S, Sakamoto M, Matsui K, Yamaguchi A, Okuhara D, Furutani S, Sattelle DB, Matsuda K (2018) Loops D, E and G in the *Drosophila* Dalpha1 subunit contribute to high neonicotinoid sensitivity of Dalpha1-chicken beta2 nicotinic acetylcholine receptor. Br J Pharmacol 175:1999–2012.

Ishii A, Shioda M, Okumura A, Kidokoro H, Sakauchi M, Shimada S, Shimizu T, Osawa M, Hirose S, Yamamoto T (2013) A recurrent KCNT1 mutation in two sporadic cases with malignant migrating partial seizures in infancy. Gene 531:467–471.

Jan YN, Jan LY (1978) Genetic dissection of short-term and long-term facilitation at the Drosophila neuromuscular junction. Proc. Natl. Acad. Sci 75:515–519.

Jiang C, Haddad GG (1993) Short periods of hypoxia activate a K^+ current in central neurons. Brain Res 614:352–356.

Kameyama M, Kakei M, Sato R, Shibasaki T, Matsuda H, Irisawa H (1984) Intracellular Na^+ activates a K^+ channel in mammalian cardiac cells. Nature 309:354–356.

Kearney JA, Plummer NW, Smith MR, Kapur J, Cummins TR, Waxman SG, Goldin AL, Meisler MH (2001) A gain-of-function mutation in the sodium channel gene Scn2a results in seizures and behavioral abnormalities. Neuroscience 102:307–317.

Kim GE, Kronengold J, Barcia G, Quraishi IH, Martin HC, Blair E, Taylor JC, Dulac O, Colleaux L, Nabbout R, Kaczmarek LK (2014) Human slack potassium channel mutations increase positive cooperativity between individual channels. Cell Rep 9:1661–1672.

Kuchibhotla KV, Goldman ST, Lattarulo CR, Wu HY, Hyman BT, Bacskai BJ (2008) Abeta plaques lead to aberrant regulation of calcium homeostasis in vivo resulting in structural and functional disruption of neuronal networks. Neuron 59:214–225.

Kuebler D, Tanouye MA (2000) Modifications of seizure susceptibility in *Drosophila*. J Neurophysiol 83:998–1009.

Kuebler D, Zhang H, Ren X, Tanouye MA (2001) Genetic suppression of seizure susceptibility in *Drosophila*. J Neurophysiol 86:1211–1225.

Kuo JJ, Schonewille M, Siddique T, Schults AN, Fu R, Bar PR, Anelli R, Heckman CJ, Kroese AB (2004) Hyperexcitability of cultured spinal motoneurons from presymptomatic ALS mice. J Neurophysiol 91:571–575.

Lee J, Wu CF (2002) Electroconvulsive seizure behavior in *Drosophila*: analysis of the physiological repertoire underlying a stereotyped action pattern in bang-sensitive mutants. J Neurosci 22:11065–11079.

Lee JM, Zipfel GJ, Choi DW (1999) The changing landscape of ischaemic brain injury mechanisms. Nature 399:A7–A14.

Lee PT, Zirin J, Kanca O, Lin WW, Schulze KL, Li-Kroeger D, Tao R, Devereaux C, Hu Y, Chung V, Fang Y, He Y, Pan H, Ge M, Zuo Z, Housden BE, Mohr SE, Yamamoto S, Levis RW, Spradling AC, et al. (2018) A gene-specific T2A-GAL4 library for *Drosophila*. Elife 7:e35574.

Lin WH, Gunay C, Marley R, Prinz AA, Baines RA (2012) Activity-dependent alternative splicing increases persistent sodium current and promotes seizure. J Neurosci 32:7267–7277.

Lossin C, Wang DW, Rhodes TH, Vanoye CG, George AL Jr (2002) Molecular basis of an inherited epilepsy. Neuron 34:877–884.

Lu R, Bausch AE, Kallenborn-Gerhardt W, Stoetzer C, Debruin N, Ruth P, Geisslinger G, Leffler A, Lukowski R, Schmidtko A (2015) Slack channels expressed in sensory neurons control neuropathic pain in mice. J Neurosci 35:1125–1135.

Lu S, Das P, Fadool DA, Kaczmarek LK (2010) The slack sodium-activated potassium channel provides a major outward current in olfactory neurons of $Kv1.3^{-/-}$ super-smeller mice. J Neurophysiol 103:3311–3319.

Luk HN, Carmeliet E (1990) Na(+)-activated K^+ current in cardiac cells: rectification, open probability, block and role in digitalis toxicity. Pflugers Arch 416:766–768.

Mao X, Bruneau N, Gao Q, Becq H, Jia Z, Xi H, Shu L, Wang H, Szepetowski P, Aniksztejn L (2020) The epilepsy of infancy with migrating focal seizures: identification of de novo mutations of the KCNT2 gene that exert inhibitory effects on the corresponding heteromeric KNa1.1/KNa1.2 potassium channel. Front Cell Neurosci 14:1.

Marley R, Baines RA (2011) Increased persistent Na^+ current contributes to seizure in the slamdance bang-sensitive *Drosophila* mutant. J Neurophysiol 106:18–29.

Martinez-Espinosa PL, Wu J, Yang C, Gonzalez-Perez V, Zhou H, Liang H, Xia XM, Lingle CJ (2015) Knockout of Slo2.2 enhances itch, abolishes KNa current, and increases action potential firing frequency in DRG neurons. Elife 4:e10013.

McGuire SE, Le PT, Davis RL (2001) The role of *Drosophila* mushroom body signaling in olfactory memory. Science 293:1330–1333.

McTague A, Nair U, Malhotra S, Meyer E, Trump N, Gazina EV, Papandreou A, Ngoh A, Ackermann S, Ambegaonkar G, Appleton R, Desurkar A, Eltze C, Kneen R, Kumar AV, Lascelles K, Montgomery T, Ramesh V, Samanta R, Scott RH, et al. (2018) Clinical and molecular characterization of KCNT1-related severe early-onset epilepsy. Neurology 90:e55–e66.

Metaxakis A, Oehler S, Klinakis A, Savakis C (2005) Minos as a genetic and genomic tool in *Drosophila melanogaster*. Genetics 171:571–581.

Milligan CJ, Li M, Gazina EV, Heron SE, Nair U, Trager C, Reid CA, Venkat A, Younkin DP, Dlugos DJ, Petrovski S, Goldstein DB, Dibbens LM,

Scheffer IE, Berkovic SF, Petrou S (2014) KCNT1 gain of function in 2 epilepsy phenotypes is reversed by quinidine. Ann Neurol 75:581–590.
Min BI, Kim CJ, Rhee JS, Akaike N (1996) Modulation of glycine-induced chloride current in acutely dissociated rat periaqueductal gray neurons by mu-opioid agonist DAGO. Brain Res 734:72–78.
Minkeviciene R, Rheims S, Dobszay MB, Zilberter M, Hartikainen J, Fulop L, Penke B, Zilberter Y, Harkany T, Pitkanen A, Tanila H (2009) Amyloid beta-induced neuronal hyperexcitability triggers progressive epilepsy. J Neurosci 29:3453–3462.
Mitani A, Shattock MJ (1992) Role of Na-activated K channel, Na-K-Cl co-transport, and Na-K pump in [K]e changes during ischemia in rat heart. Am J Physiol 263:H333–H340.
Møller RS, Heron SE, Larsen LH, Lim CX, Ricos MG, Bayly MA, van Kempen MJ, Klinkenberg S, Andrews I, Kelley K, Ronen GM, Callen D, McMahon JM, Yendle SC, Carvill GL, Mefford HC, Nabbout R, Poduri A, Striano P, Baglietto MG, et al. (2015) Mutations in KCNT1 cause a spectrum of focal epilepsies. Epilepsia 56:e114–e120.
Nanou E, El Manira A (2007) A postsynaptic negative feedback mediated by coupling between AMPA receptors and Na^+-activated K^+ channels in spinal cord neurones. Eur J Neurosci 25:445–450.
Palop JJ, Chin J, Roberson ED, Wang J, Thwin MT, Bien-Ly N, Yoo J, Ho KO, Yu GQ, Kreitzer A, Finkbeiner S, Noebels JL, Mucke L (2007) Aberrant excitatory neuronal activity and compensatory remodeling of inhibitory hippocampal circuits in mouse models of Alzheimer's disease. Neuron 55:697–711.
Parker L, Howlett IC, Rusan ZM, Tanouye MA (2011a) Seizure and epilepsy: studies of seizure disorders in *Drosophila*. Int Rev Neurobiol 99:1–21.
Parker L, Padilla M, Du Y, Dong K, Tanouye MA (2011b) *Drosophila* as a model for epilepsy: bss is a gain-of-function mutation in the para sodium channel gene that leads to seizures. Genetics 187:523–534.
Pavlidis P, Tanouye MA (1995) Seizures and failures in the giant fiber pathway of *Drosophila* bang-sensitive paralytic mutants. J Neurosci 15:5810–5819.
Pavlidis P, Ramaswami M, Tanouye MA (1994) The *Drosophila* easily shocked gene: a mutation in a phospholipid synthetic pathway causes seizure, neuronal failure, and paralysis. Cell 79:23–33.
Perozo E, MacKinnon R, Bezanilla F, Stefani E (1993) Gating currents from a nonconducting mutant reveal open-closed conformations in Shaker K^+ channels. Neuron 11:353–358.
Perry T, Heckel DG, McKenzie JA, Batterham P (2008) Mutations in Dalpha1 or Dbeta2 nicotinic acetylcholine receptor subunits can confer resistance to neonicotinoids in *Drosophila melanogaster*. Insect Biochem Mol Biol 38:520–528.
Perry T, Chan JQ, Batterham P, Watson GB, Geng C, Sparks TC (2012) Effects of mutations in Drosophila nicotinic acetylcholine receptor subunits on sensitivity to insecticides targeting nicotinic acetylcholine receptors. Pestic Biochem Physiol 102:56–60.
Ping Y, Tsunoda S (2011) Inactivity-induced increase in nAChRs upregulates Shal K(+) channels to stabilize synaptic potentials. Nat Neurosci 15:90–97.
Ping Y, Waro G, Licursi A, Smith S, Vo-Ba DA, Tsunoda S (2011) Shal/K(v)4 channels are required for maintaining excitability during repetitive firing and normal locomotion in *Drosophila*. PLoS One 6:e16043.
Ping Y, Hahm ET, Waro G, Song Q, Vo-Ba DA, Licursi A, Bao H, Ganoe L, Finch K, Tsunoda S (2015) Linking abeta42-induced hyperexcitability to neurodegeneration, learning and motor deficits, and a shorter lifespan in an Alzheimer's model. PLoS Genet 11:e1005025.
Quraishi IH, Stern S, Mangan KP, Zhang Y, Ali SR, Mercier MR, Marchetto MC, McLachlan MJ, Jones EM, Gage FH, Kaczmarek LK (2019) An epilepsy-associated KCNT1 mutation enhances excitability of human iPSC-derived neurons by increasing Slack KNa currents. J Neurosci 39:7438–7449.
Quraishi IH, Mercier MR, McClure H, Couture RL, Schwartz ML, Lukowski R, Ruth P, Kaczmarek LK (2020) Impaired motor skill learning and altered seizure susceptibility in mice with loss or gain of function of the Kcnt1 gene encoding Slack (KNa1.1) Na(+)-activated K(+) channels. Sci Rep 10:3213.
Ravenscroft TA, Janssens J, Lee PT, Tepe B, Marcogliese PC, Makhzami S, Holmes TC, Aerts S, Bellen HJ (2020) *Drosophila* voltage-gated sodium channels are only expressed in active neurons and are localized to distal axonal initial segment-like domains. J Neurosci 40:7999–8024.
Rizzi S, Knaus HG, Schwarzer C (2016) Differential distribution of the sodium-activated potassium channels slick and slack in mouse brain. J Comp Neurol 524:2093–2116.
Rizzo F, Ambrosino P, Guacci A, Chetta M, Marchese G, Rocco T, Soldovieri MV, Manocchio L, Mosca I, Casara G, Vecchi M, Taglialatela M, Coppola G, Weisz A (2016) Characterization of two de novo KCNT1 mutations in children with malignant migrating partial seizures in infancy. Mol Cell Neurosci 72:54–63.
Somers J, Nguyen J, Lumb C, Batterham P, Perry T (2015) In vivo functional analysis of the Drosophila melanogaster nicotinic acetylcholine receptor Dα6 using the insecticide spinosad. Insect Biochem Mol Biol 64:116–127.
Song J, Tanouye MA (2008) From bench to drug: human seizure modeling using *Drosophila*. Prog Neurobiol 84:182–191.
Strother JA, Wu ST, Wong AM, Nern A, Rogers EM, Le JQ, Rubin GM, Reiser MB (2017) The emergence of directional selectivity in the visual motion pathway of *Drosophila*. Neuron 94:168–182.e110.
Sun L, Gilligan J, Staber C, Schutte RJ, Nguyen V, O'Dowd DK, Reenan R (2012) A knock-in model of human epilepsy in *Drosophila* reveals a novel cellular mechanism associated with heat-induced seizure. J Neurosci 32:14145–14155.
Tamsett TJ, Picchione KE, Bhattacharjee A (2009) NAD^+ activates KNa channels in dorsal root ganglion neurons. J Neurosci 29:5127–5134.
Tanaka NK, Tanimoto H, Ito K (2008) Neuronal assemblies of the *Drosophila* mushroom body. J Comp Neurol 508:711–755.
Tang QY, Zhang FF, Xu J, Wang R, Chen J, Logothetis DE, Zhang Z (2016) Epilepsy-related Slack channel mutants lead to channel over-activity by two different mechanisms. Cell Rep 14:129–139.
Tomasello DL, Hurley E, Wrabetz L, Bhattacharjee A (2017) Slick (Kcnt2) sodium-activated potassium channels limit peptidergic nociceptor excitability and hyperalgesia. J Exp Neurosci 11:1179069517726996.
Tsunoda S, Salkoff L (1995a) Genetic analysis of *Drosophila* neurons: shal, Shaw, and Shab encode most embryonic potassium currents. J Neurosci 15:1741–1754.
Tsunoda S, Salkoff L (1995b) The major delayed rectifier in both *Drosophila* neurons and muscle is encoded by Shab. J Neurosci 15:5209–5221.
van Swinderen B (2009) Fly memory: a mushroom body story in parts. Curr Biol 19:R855–R857.
Vanoye CG, Lossin C, Rhodes TH, George AL Jr (2006) Single-channel properties of human NaV1.1 and mechanism of channel dysfunction in SCN1A-associated epilepsy. J Gen Physiol 127:1–14.
Venken KJ, Schulze KL, Haelterman NA, Pan H, He Y, Evans-Holm M, Carlson JW, Levis RW, Spradling AC, Hoskins RA, Bellen HJ (2011) MiMIC: a highly versatile transposon insertion resource for engineering *Drosophila melanogaster* genes. Nat Methods 8:737–743.
Yuan A, Dourado M, Butler A, Walton N, Wei A, Salkoff L (2000) SLO-2, a K^+ channel with an unusual Cl^- dependence. Nat Neurosci 3:771–779.
Yuan A, Santi CM, Wei A, Wang ZW, Pollak K, Nonet M, Kaczmarek L, Crowder CM, Salkoff L (2003) The sodium-activated potassium channel is encoded by a member of the Slo gene family. Neuron 37:765–773.
Zhang H, Tan J, Reynolds E, Kuebler D, Faulhaber S, Tanouye M (2002) The *Drosophila* slamdance gene: a mutation in an aminopeptidase can cause seizure, paralysis and neuronal failure. Genetics 162:1283–1299.